CHAPTER IV

RESULTS AND DISCUSSION

Effect of Eu concentrations in ZrO_2 with fixed Y (ZrO_2: 7%Y: x%Eu)

1. Crystal structure of ZrO_2: 7%Y: x%Eu

Figure 31 shows the XRD pattern of the ZrO_2 crystal co-doped with Y and Eu under calcination at 800 °C for 1 h. The concentration of Eu^{3+} ion was varied from 1 to 10 mol% while the content of Y was fixed at 7 mol%. The diffraction pattern of ZrO_2 without the dopant presents the monoclinic phase as can be seen from Figure 31a. When 1 mol% of Eu is introduced into the ZrO_2 crystal (Figure 31b), the monoclinic phase transforms to the tetragonal phase. The crystal still has a fraction of monoclinic phase as indicated by the (-111) reflection plane at $2\theta = 28°$. When Eu concentration is increased to 3 mol%, only tetragonal phase is obtained. It can be seen that the sharp peaks appear at $2\theta = 30.27$, 35.26, 50.38 and 60.1°, which correspond to the (111), (002), (200), (220), (202), (113) and (311) reflection plane of tetragonal structure of the crystalline ZrO_2. The doping of Y (7 mol%) into ZrO_2 crystal resulted in the formation of cubic phase as shown in Figure 31d. The discrepancy between cubic and tetragonal phase can be clearly observed at $2\theta = 35.26$, 50.38 and 60.1° where the splitted peaks of tetragonal phase disappear as shown in Figure 32. The doping of 1 and 3 mol% Eu into ZrO_2 crystal with 7 mol% of Y still provided the cubic phase. From the results, we can see that the doping of ZrO_2 crystal with Y and Eu leads to the phase transformation.

The crystal size can be estimated from the line width of XRD peaks by using the Scherrer formular as described in chapter 3. The crystal size of ZrO_2: 7%Y doped with various concentrations of Eu ranging from 1, 2, 3, 4, 6 and 8 to 10 mol% was calculated and summarized in Table 1. It was found that the crystal size of ZrO_2 was 30.2 nm. When 1 mol% of Eu and 7 mol% of Y are introduced into the ZrO_2 crystal, the crystal size is 21.6 and 12.1 nm, respectively. The decrease of crystal size is probably due to the smaller atomic radius of Zr compared to those of Eu and Y. For

the crystal size of ZrO_2: 7%Y doped with various concentrations of Eu at 1 and 10 mol%, the crystal size decreases with increasing of concentration of Eu.

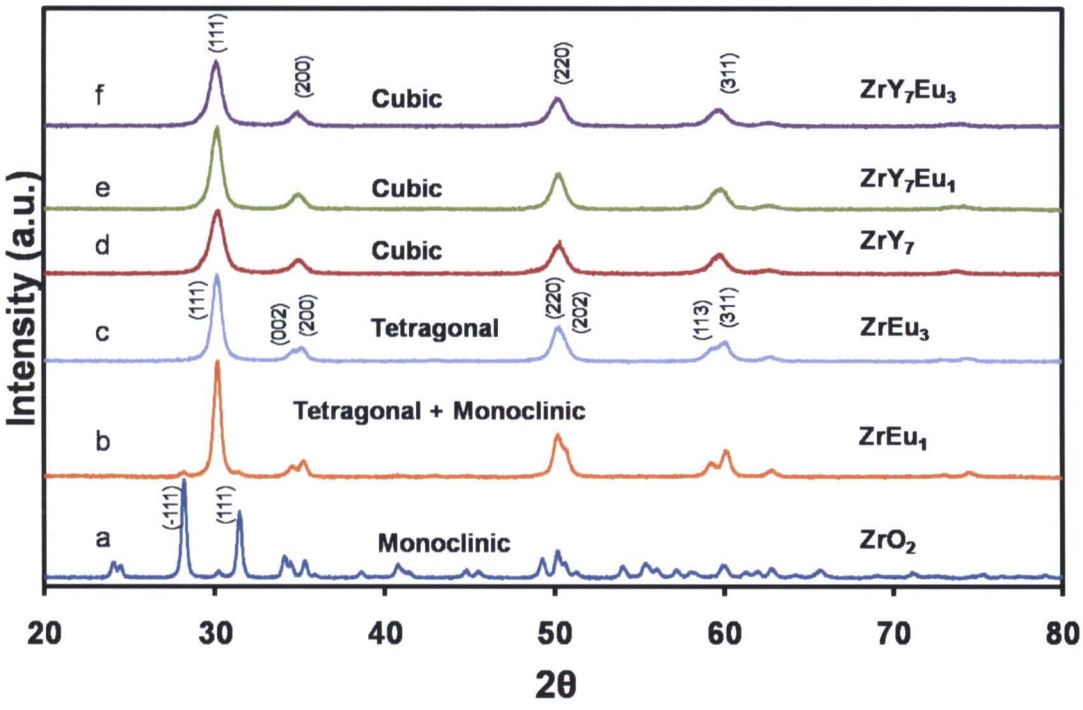

Figure 31 Powder XRD patterns of ZrO_2: 7%Y crystals doped with various concentrations of Eu under calcination at 800 °C for 1 h

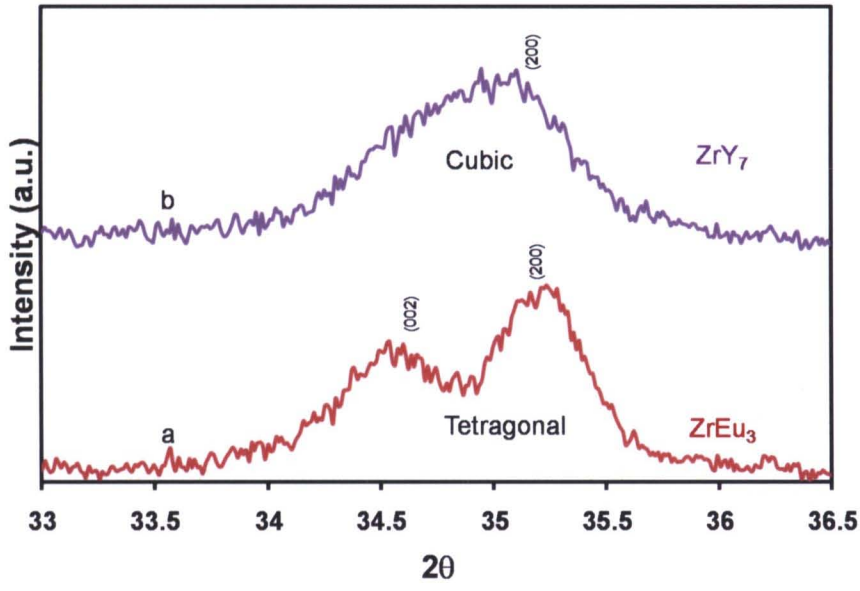

Figure 32 XRD patterns of (a) ZrO_2: 3%Eu and (b) ZrO_2: 7%Y crystal under calcination at 800 °C for 1

Table 1 The crystal size of ZrO_2: 7mol%Y crystal doped with various concentration of Eu under calcination at 800 °C for 1 h as calculated from XRD line width

Samples	Crystal size (nm)
ZrO_2	30.2
$ZrEu_1$	21.6
ZrY_7	12.1
ZrY_7Eu_1	13.8
ZrY_7Eu_2	12.1
ZrY_7Eu_3	12.1
ZrY_7Eu_4	10.8
ZrY_7Eu_6	10.8
ZrY_7Eu_8	10.8
ZrY_7Eu_{10}	9.7

The change of crystal size can be clearly seen from the normalized peak of XRD spectra at (111) reflection plane. The normalized peaks of ZrO_2: 7%Y crystal doped with various concentrations of Eu ranging from 1, 2, 3, 4, 6 and 8 to 10 mol% are shown in Figure 33. It was found that the normalized peak of 1 mol% of Eu doped into the ZrO_2 crystal is sharp. The normalized peaks of ZrO_2: 7%Y doped with various concentrations of Eu at 1 and 10 mol% become broader upon increasing concentrations of Eu. The broadening of XRD peak corresponds to the decrease of crystal size.

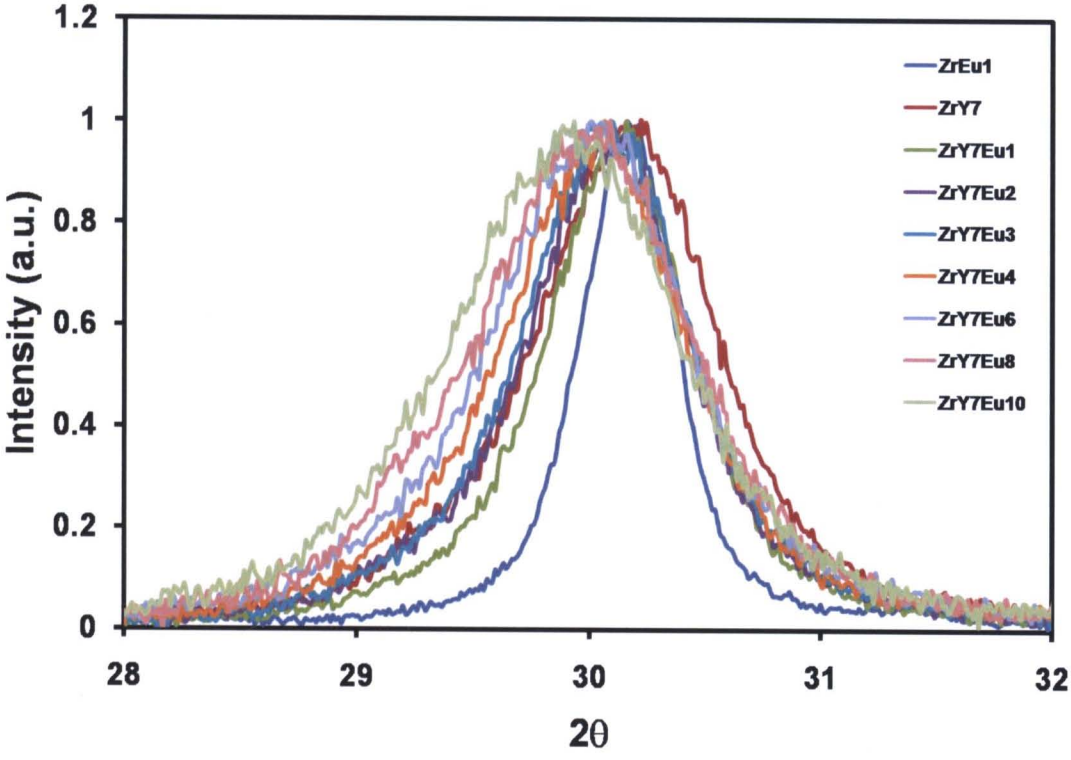

Figure 33 Normalized peaks of XRD spectra of ZrO_2: 7%Y crystals doped with various concentrations of Eu under calcination at 800 °C for 1 h

The vibrational spectroscopy was also utilized to characterize structural change of ZrO_2 crystal. The FT-IR spectra of the ZrO_2 crystal co-doped with Y and Eu were recorded in the range of 400 to 1000 cm^{-1} as shown in Figure 34. The vibrational bands of Zr-O bond mainly appear at about 400 to 800 cm^{-1}. The bands at about 418, 504, 575 and 744 cm^{-1} correspond to the monoclinic structure of ZrO_2 crystal as shown in Figure 34a. When the monoclinic phase transforms to tetragonal phase in $ZrEu_3$, the vibrational bands change significantly [44]. The broad band with two peaks at about 480 and 750 cm^{-1} were detected (see Figure 34b). In cubic phase of ZrY_7, ZrY_7Eu_1 and ZrY_7Eu_3 crystals broad band ranging from 550 to 750 cm^{-1} was observed as shown in Figure 34c – 34e. The results obtained from the XRD and FT-IR indicates that the doping of Eu and Y into ZrO_2 crystal causes the formation of cubic phase.

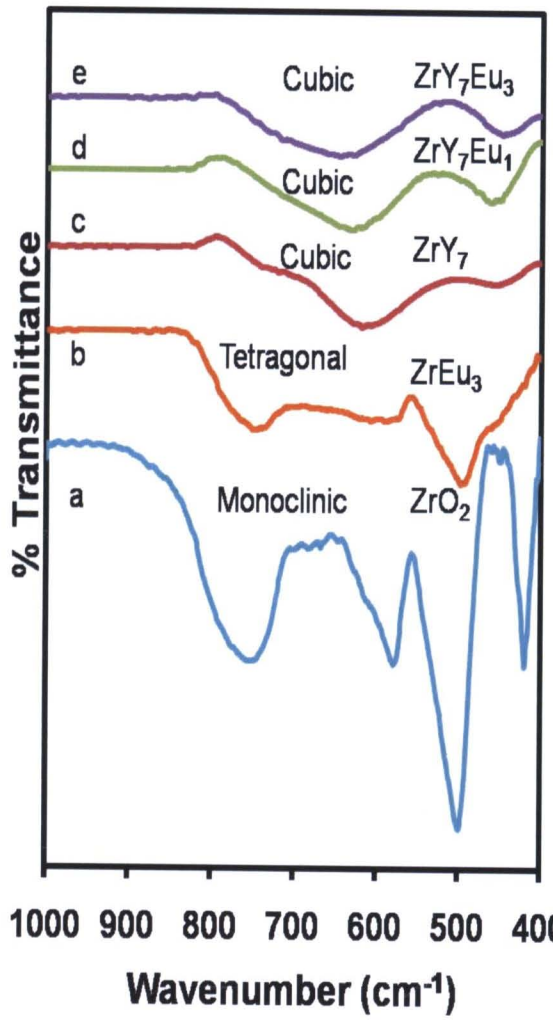

Figure 34 FT-IR spectra of ZrO_2: 7%Y crystals doped with various concentrations of Eu under calcination at 800 °C for 1 h

2. Morphology of ZrO_2: 7%Y: x%Eu crystals

Figure 35 displays the SEM photograph of ZrO_2 crystal doped with Eu and Y under calcination at 800 °C for 1 h. The pure ZrO_2 crystal exhibits irregular shape particles with dimension of about 8 μm. The higher magnification image reveals densely packed particles with much smaller diameter ranging from 150-200 nm (see Figure 35b). The morphology of Eu and Y doped ZrO_2 crystal also exhibits irregular shape particles with dimension comparable to that of the pure ZrO_2.

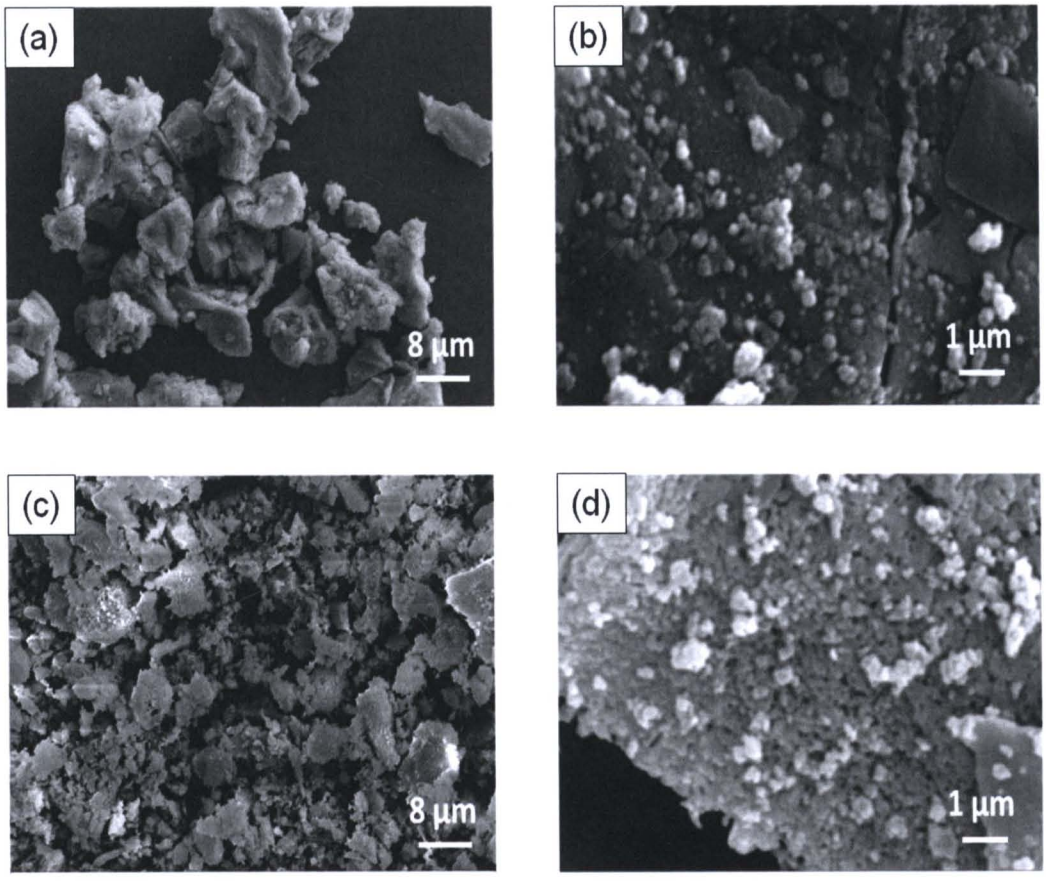

Figure 35 SEM images of ZrO_2 (a, b) and ZrO_2: 7%Y: 3%Eu (c, d) crystals under calcinations at 800 °C for 1 h

3. Luminescence properties of ZrO_2 : 7%Y : x%Eu crystals

Figure 36 shows the excitation spectra for Eu and Y doped ZrO_2 crystals by monitoring the emission at 610 nm. The excitation spectra of ZrO_2 and ZrY_7 crystals are not detected (Figure 36a, 36b). When 1 mol% of Eu is introduced into the ZrO_2 crystal, the excitation spectrum consists of a strong band at 229, 246, 260 and 394 nm as shown in Figure 36c. The doping of Y into ZrO_2: 1%Eu and ZrO_2: 3%Eu crystals, the spectra still appear at four bands and the intensity increase with increasing of Eu concentrations (Figure 36d, 36e). The excitation spectrum at wavelength in range of 229 to 260 nm might be ascribed to the host absorption of the oxygen-to-europium charge transfer band (CTB) at UV region. As mentioned in the chapter I, the charge transfer occurs via the transition from 2p orbital of O^{2-} ions to the 4f orbital of Eu^{3+} ions [55]. These excitation spectra suggest that most of the Eu^{3+} ions are

substituted at Zr^{4+} sites in the ZrO_2 lattice, as indicated by the detection of the CTB band. The other weak peaks at 365, 397 and 468 nm are the direct excitation of the general f-f transitions within the $4f^6$ electron configuration of Eu.

The dependence of luminescence intensity on the excitation wavelength of the Eu doped ZrO_2 crystal suggests the energy transfer from the ZrO_2 crystal to Eu. There are two channels of excitations in the Eu. One is direct excitation of the Eu^{3+} ions, i.e., bands at about 350 to 480 nm. Another channel is the excitation of ZrO_2, i.e., excitation into the conduction band of host crystal, followed by an energy transfer from the host into the Eu^{3+} ions to cause the emission. The energy transfer between the ZrO_2 crystal and the Eu^{3+} ions is clearly observed in the excitation spectra, i.e., bands at about 200 to 350 nm, as shown in Figure 36.

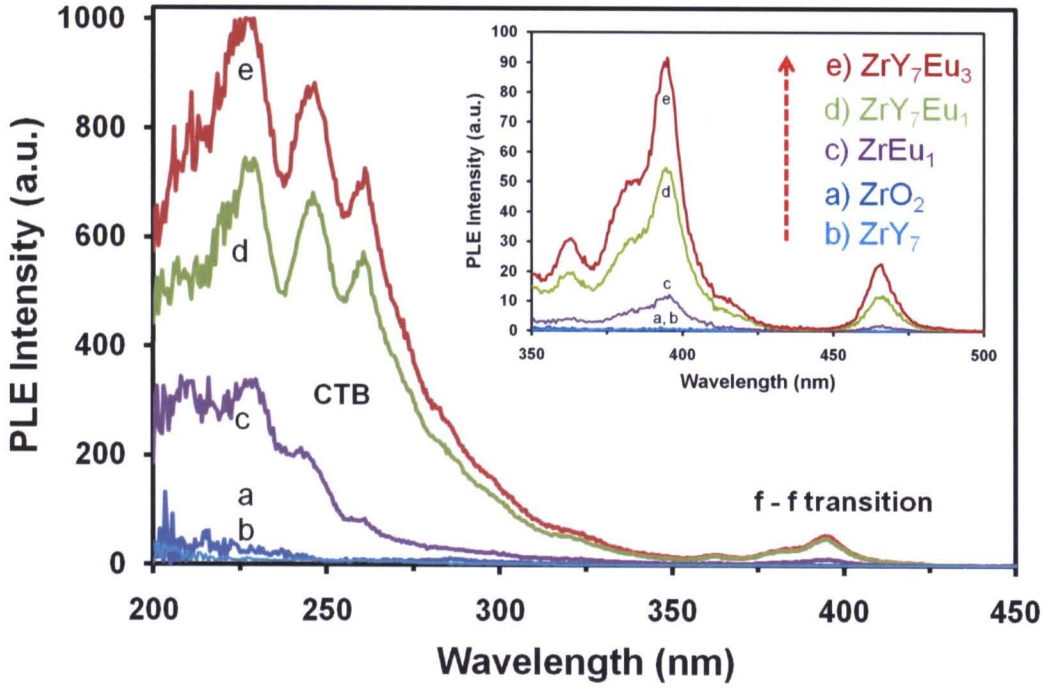

Figure 36 PL excitation spectra of ZrO_2: 7%Y crystals doped with various concentrations of Eu under calcination at 800 °C for 1 h

The photoluminescence (PL) spectra of Eu and Y doped ZrO_2 crystals under the excitation of short wavelength UV light at 260 nm are shown in Figure 37. The ZrO_2 and ZrY_7 crystals do not emit light under this excitation condition. When 1 and 3 mol% of Eu are introduced into the ZrO_2 crystal, the materials exhibit a red light

emission. These PL spectra have similar pattern and are composed of $^5D_0 - {}^7F_J$ (J=1, 2, 3, 4) emission lines of Eu. The $^5D_0 - {}^7F_2$ (607 or 610 nm) transition dominates the whole PL spectra. The emission from the higher energy levels ($^5D_1$, $^5D_2$) of Eu is not observed due to multiphoton relaxation which is able to bridge the gaps between the higher energy levels ($^5D_1$, $^5D_2$) and the lowest $^5D_0$ level effectively [70]. The doping of 1 and 3 mol% Eu into ZrO_2 crystal with 7 mol% of Y still causes the emission of red color. However, the presence of Y in the crystals causes higher emission intensity. For the crystal with 3 mol% of Eu and 7 mol% of Y, the emission intensity is highest. Our XRD results in earlier discussion also show that the presence of Y in the ZrO_2 crystal causes phase transformation. We suggest that the phase transformation is the main reason for the increase of PL intensity of Eu doped ZrO_2: 7%Y crystals. The PL intensity also varies with the Eu content.

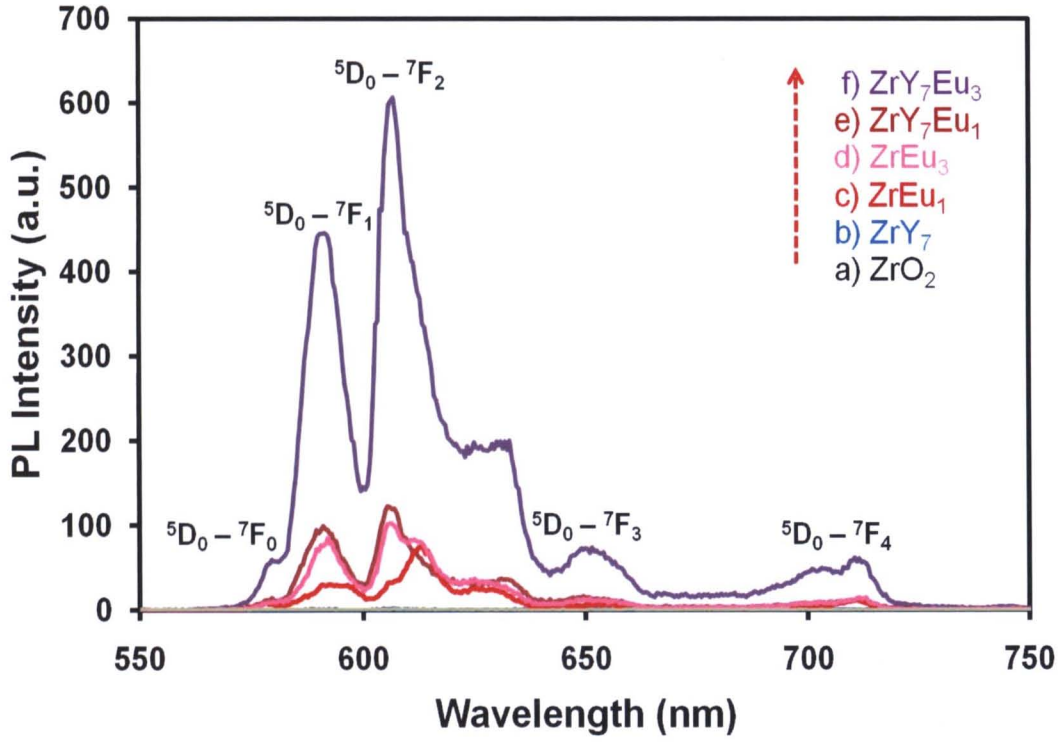

Figure 37 PL emission spectra of ZrO_2: 7%Y crystals doped with various concentrations of Eu under excitation at 260 nm

Figure 38 shows the dependence of the emission intensity on the doping concentration of Eu in ZrO_2: 7%Y crystals. The peak area was determined as an integral of PL spectrum ranging from 550 to 750 nm. It was found that the PL intensity reached maximum at 3 mol% of Eu. Further increasing Eu concentration led to rapid decrease of PL intensity. The excess Eu content affects the PL intensity via the concentration quenching process [15]. Generally, only a fraction of Eu can substitute into the ZrO_2 host lattice. The rest may adsorb at the surface of ZrO_2 host lattice, which results in the concentration quenching. The phenomenon of concentration quenching can be described to cross-relaxation process in close Eu - Eu pairs. The effect of Y in the ZrO_2 crystal on luminescence property was also clearly observed. The PL intensities of ZrO_2 crystals doped with various concentrations of Eu ranging from 1 to 3 mol% were measured and compared with those of ZrO_2: 7%Y:xEu system. It is obvious that the PL intensity of ZrO_2: 7%Y: x%Eu is higher in all Eu concentration. As mentioned above, the doping of Y into ZrO_2 crystals causes phase transformation, which can greatly promote the luminescent efficiency of samples.

The photoluminescence of the materials can be clearly seen by naked eyes under UV light irradiation as shown in Figure 39. Prior to the irradiation, all samples exhibit a white color. When excited under UV light, the ZrO_2 and ZrO_2: 7%Y crystals emit green color. On the other hand, the ZrO_2: 7%Y crystals doped with various concentrations of Eu ranging from 1 to 6 mol% emit red color.

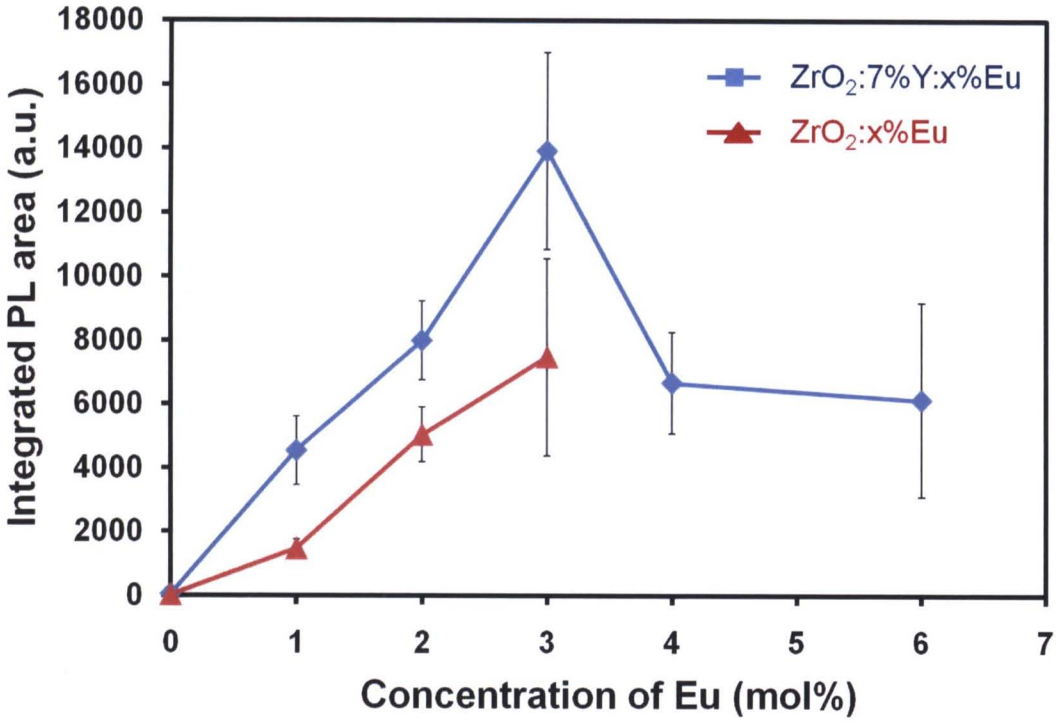

Figure 38 Integrated PL intensities of the ZrO_2: 7%Y crystals doped with various concentrations of Eu ranging from 1 to 6 mol% (◆) and ZrO_2 crystals doped with various concentrations of Eu ranging from 1 to 3 mol% (▲) under calcination at 800 °C for 1 h

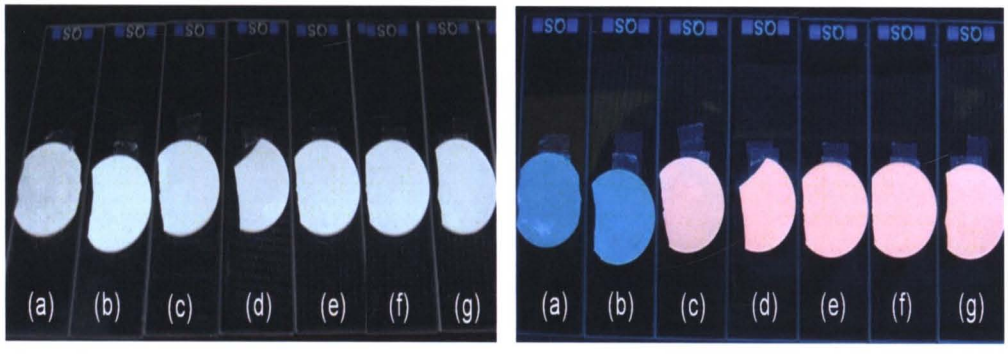

Figure 39 Photographs of the sample of ZrO_2: 7%Y crystals with various concentrations of Eu ranging from 1 to 6 mol% (left) prior to the irradiation and (right) under UV light irradiation (a) ZrO_2, (b) ZrO_2: 7%Y and (c-d) ZrO_2: 7%Y: x%Eu; x = 1, 2, 3, 4, 6 mol%

Effect of Y concentrations in ZrO_2 with fixed Eu (ZrO_2: x%Y: 3%Eu)

1. Crystal structure of ZrO_2: x%Y: 3%Eu crystals

In our earlier discussion, ZrO_2 crystals doped with 7 mol% of Y and 3 mol% of Eu exhibit the highest PL intensity. The variation of Y content may also affect the crystal structure and PL efficiency of the materials. Therefore, this section investigates the effects of Y. The quantity of Eu was fixed at 3 mol% whereas the ratio of Y was varied from 0 to 7 mol% (ZrO_2: x%Y: 3%Eu). The crystals were obtained by calcination at 800 °C for 1 h. The phase transformation of ZrO_2: 3% doped with various concentration of Y was investigated by XRD. The diffraction pattern of ZrO_2 crystal without the dopant presents the monoclinic phase as can be seen from Figure 40a. When 3 mol% of Eu is introduced into the ZrO_2 crystal, the monoclinic phase transform to tetragonal phase as shown in Figure 40b. It can be seen that the sharp peaks appear at 2θ = 30.27, 35.26, 50.38 and 60.1°, which corresponds to the (111), (002), (200), (220), (113) and (311) reflection plane of tetragonal structure of the crystalline ZrO_2. Then, the Y was introduced into the ZrO_2 crystal with fixed content of Eu at 3 mol%. The doping of 1 mol% Y causes the transformation of the structure from tetragonal to cubic phase as shown in Figure 40c. The increase of Y content from 1 to 7 mol% still yields the cubic phase. From the results, we can see that the doping of ZrO_2 crystal with Y and Eu leads to the phase transformation.

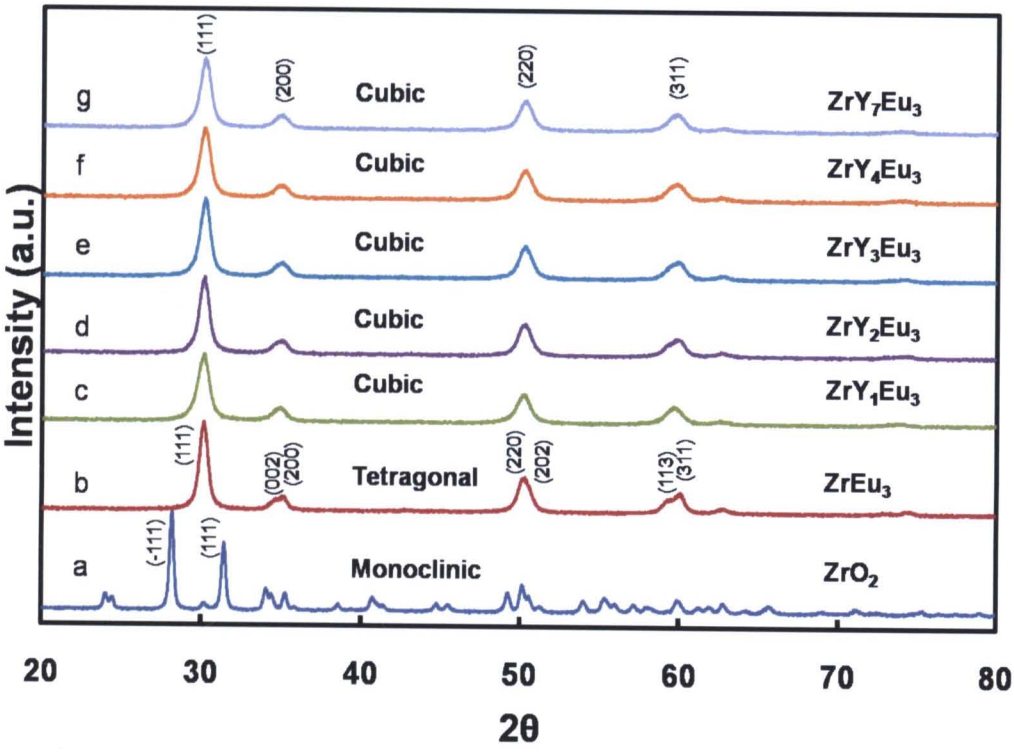

Figure 40 Powder XRD patterns of ZrO_2: 3%Eu doped with various concentrations of Y ranging from 1 to 7 mol% under calcination at 800 °C for 1 h

The average crystal size of the sample was determined from the line width of XRD peaks by using the Scherrer formular. The crystal size of ZrO_2: 3%Eu doped with various concentrations of Y ranging from 0, 1, 2, 3, and 4, 5 to 7 mol% can be calculated and summarized in Table 2. It was found that the crystal size of ZrO_2 crystal doped with 3 mol% of Eu is 16.2 nm. When 1 mol% of Y is introduced into ZrO_2: 3%Eu crystal, the crystal size is 13.8 nm. The crystal sizes hardly change when the Y concentration in ZrO_2: 3%Eu crystal is increased to 7 mol%.

The normalized peaks of ZrO_2: 3%Eu doped with various concentrations of Y ranging from 0, 1, 2, 3, and 4, 5 to 7 mol% are shown in Figure 41. The normalized peak of ZrO_2 crystal doped with 3 mol% of Eu is broad. When the ZrO_2: 3%Eu crystal is doped with 1 mol% of Y, the peak is broader. The increase of Y content from 2 to 7 mol% causes slight increase of the peak width.

Table 2 The crystal size of ZrO_2: 3%Eu crystal doped with various concentration of Y under calcination at 800 °C for 1 h as calculated from XRD line width

Samples	Crystal size (nm)
$ZrEu_3$	16.2
ZrY_1Eu_3	13.8
ZrY_2Eu_3	13.8
ZrY_3Eu_3	13.8
ZrY_4Eu_3	12.9
ZrY_5Eu_3	12.1
ZrY_7Eu_3	12.1

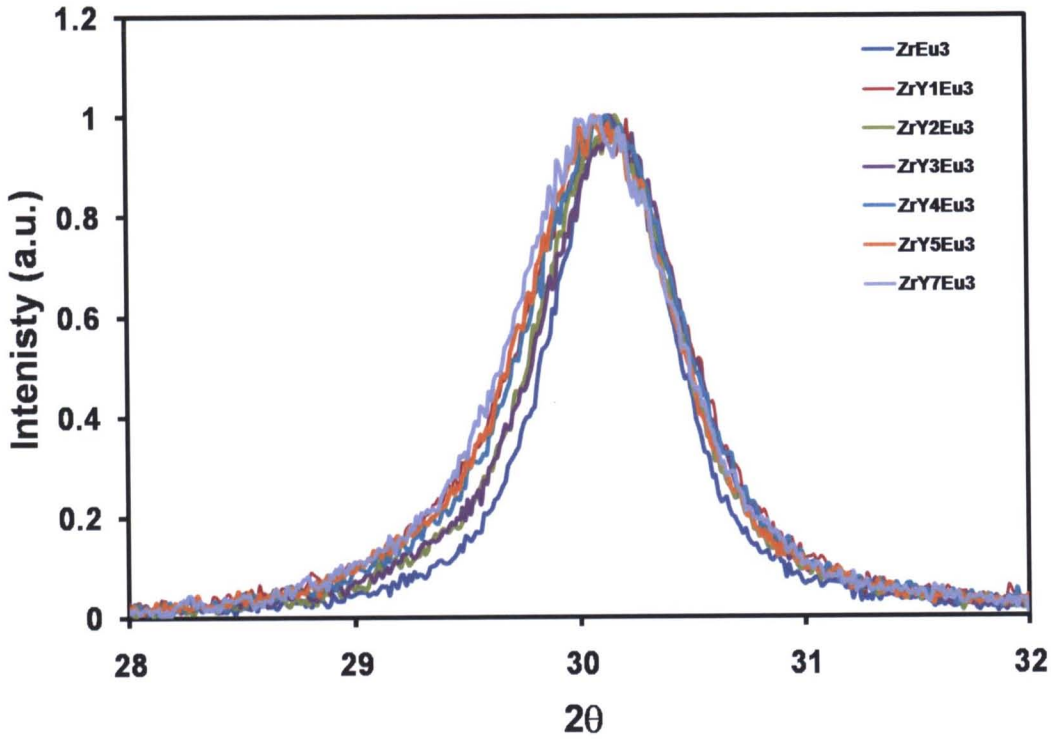

Figure 41 The normalized peak of XRD spectra of ZrO_2: 3%Eu doped with various concentrations of Y ranging from 1 to 7 mol% under calcination at 800 °C for 1 h

2. Morphology of ZrO_2: x%Y: 3%Eu crystals

The SEM photographs of ZrO_2: 3%Eu doped with various concentration of Y under calcination at 800 °C for 1 h are shown in Figure 42. The ZrO_2: 3%Eu crystal with doping concentrations of Y at 1, 3 and 7 mol% exhibit similar shape. The dimension of irregular shape particles is in the micron range (see Figure 42a, 42c and 42e). The higher magnification images also show the smaller particles, densely packed within the large particles. The average grain size is about 150-200 nm as shown in Figure 42b, 42d and 42f. The result indicates that the amount of Y concentration in ZrO_2: 3%Eu crystal has slight effects on particle size and characteristics of crystals.

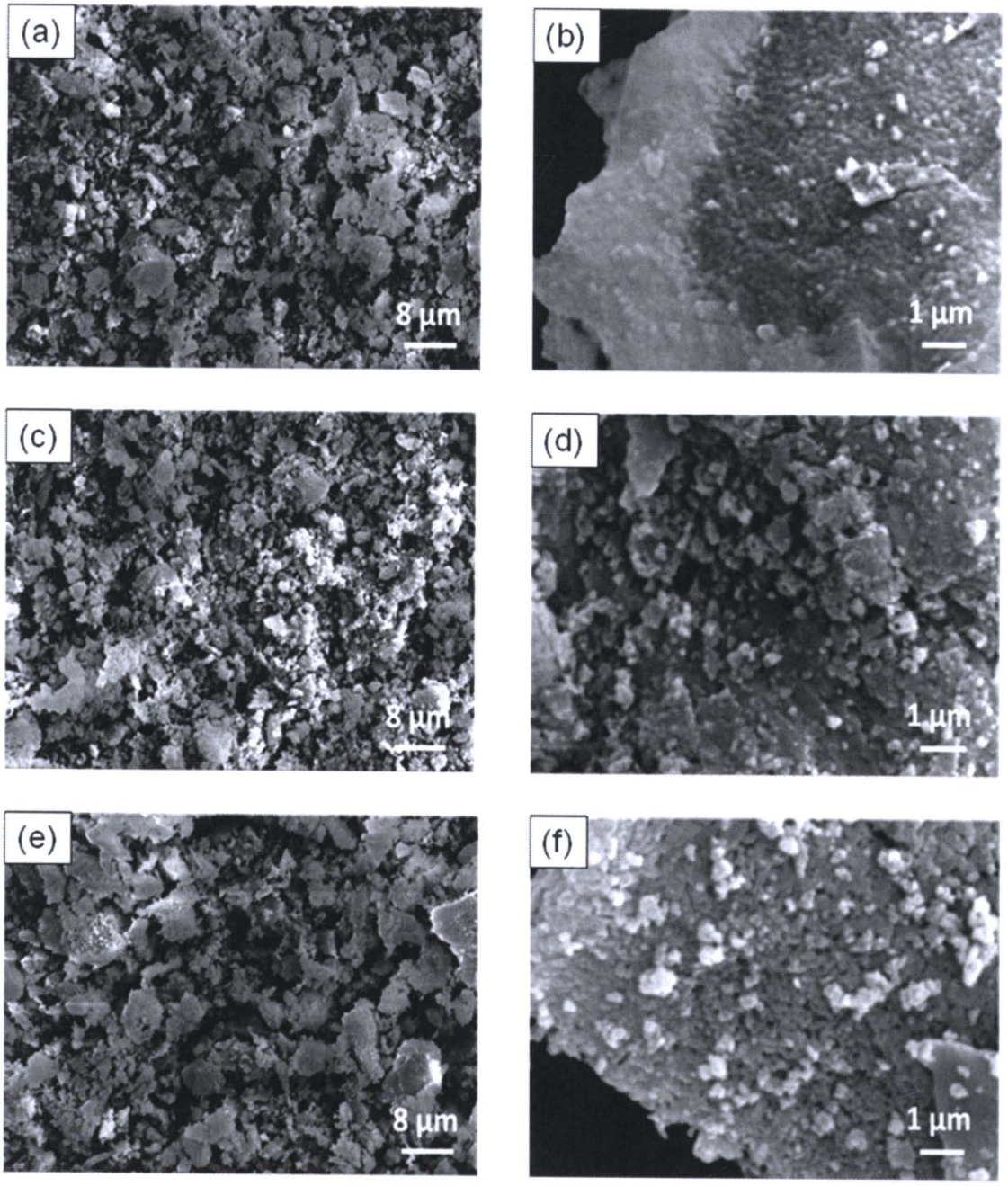

Figure 42 SEM images of ZrO_2: 3%Eu crystal doped with various concentrations of Y under calcination at 800 °C for 1 h (a, b) ZrO_2: 3%Eu: 1%Y, (c, d) ZrO_2: 3%Eu: 3%Y and (e, f) ZrO_2: 3%Eu: 7%Y

3. Luminescence properties of ZrO_2: x%Y: 3%Eu crystals

The effect of phase transformation on optical property of ZrO_2: 3%Eu doped with various concentration of Y ranging from 0 to 7 mol% was investigated under UV excitation at 260 nm (λ_{ex} = 260 nm) as shown in Figure 43. The ZrO_2 crystals do not emit light under this excitation condition. When 3 mol% of Eu is introduced into the ZrO_2 crystal, the materials exhibit a red light emission. The doping of 1 to 7 mol% Y into ZrO_2 crystal with 3 mol% of Eu still caused the emission of red color. These PL spectra exhibited similar pattern and were composed of $^5D_0 - {}^7F_J$ (J=1, 2, 3, 4) emission lines of Eu. However, the emission intensity varied significantly with the Y concentration. The emission intensity was highest when the content of Y was increased to 4 mol%. Further increasing Y concentration caused drastic drop of emission intensity. These results indicate that the content of Y in the crystals affect the luminescence efficiency.

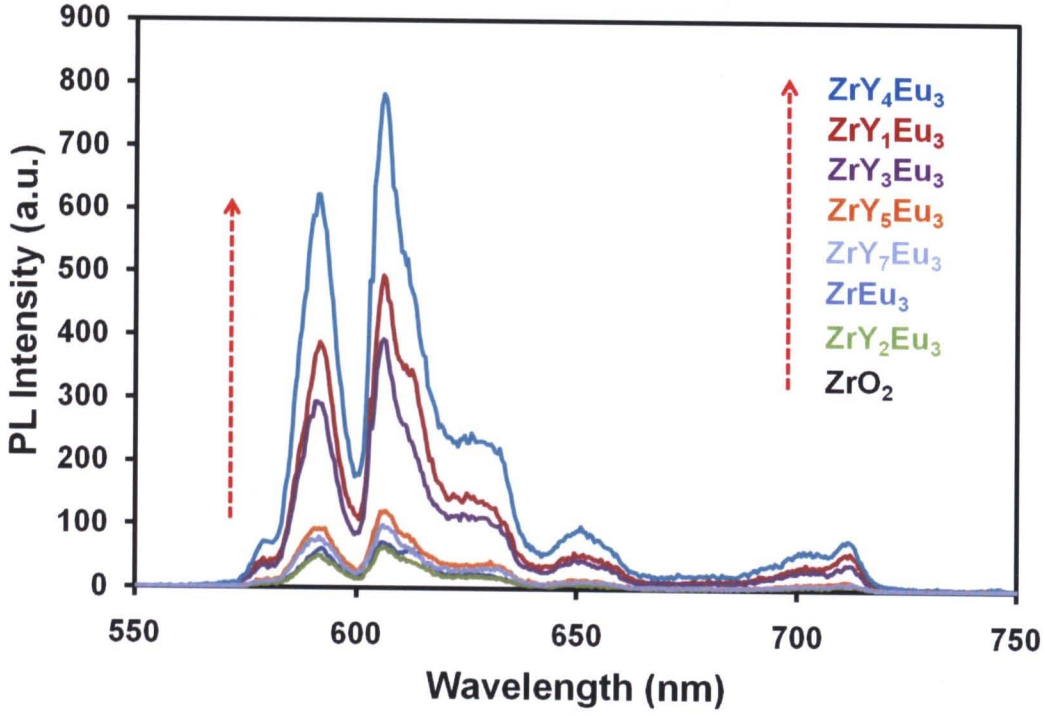

Figure 43 PL emission spectra of ZrO_2: 3%Eu crystal doped with various concentrations of Y ranging from 1 to 7 mol% under calcination at 800 °C for 1 h

To further illustrate the effect of Y on the PL intensity, we plotted the graph between PL areas and concentration of Y as shown in Figure 44. The PL areas were integrated from 550 to 750 nm. The plot clearly shows that the PL intensity increases to maximum at 4 mol% of Y. It decreases rapidly when the concentration of Y was further increased. The highest PL intensity is 5 time higher when compared to the PL intensity of the ZrO_2: 3%Eu crystal without Y. Although the crystals with Y concentration of 1 to 7 mol% exhibit the cubic phase, the materials show different luminescent properties. Therefore, the amount of Y in the crystal somehow affects the de-excitation process. However, the origin of this observation is not known and needed to be further investigated.

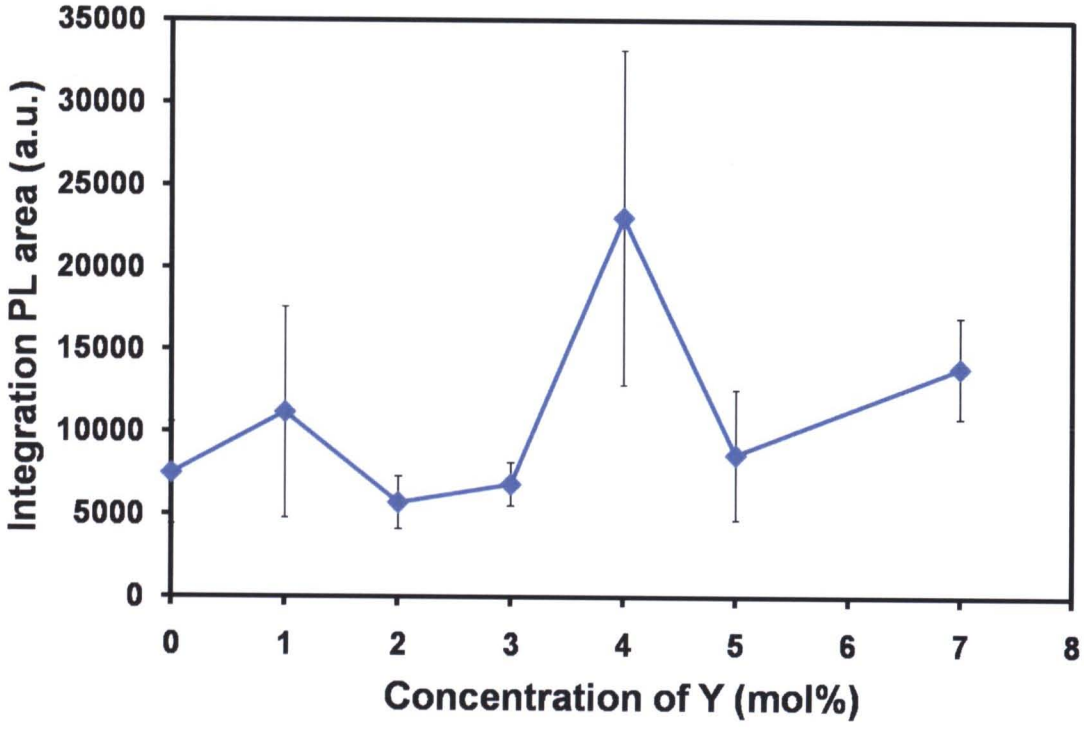

Figure 44 Integrated PL intensities of ZrO_2: 3%Eu crystal doped with various concentrations of Y ranging from 1 to 7 mol% under calcination at 800 °C for 1 h

The photoluminescence of the materials can be clearly seen by naked eyes under UV light irradiation as shown in Figure 45. Prior to the irradiation, all samples exhibit a white color. When excite under UV light, the ZrO_2 crystal emit green color.

On the other hand, the ZrO_2: 3%Eu crystal doped with various concentrations of Y ranging from 1 to 7 mol% emits red color.

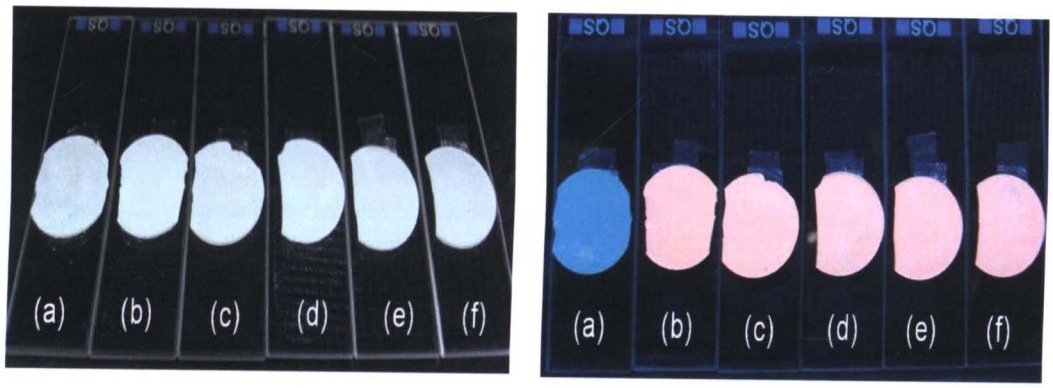

Figure 45 Photographs of the sample of ZrO_2: 3%Eu crystals doped with various concentrations of Y (left) prior to the irradiation and (right) under UV light irradiation (a) ZrO_2 and (b-f) ZrO_2: 3%Eu: x%Y, x = 0, 1, 3, 5, 7 mol%

Effect of temperatures

1. Crystal structure of ZrO_2: 4%Y: 3%Eu

The synthesis of our samples in this study requires calcinations to induce the crystallization of the materials. Therefore, the change of calcination temperatures is expected to influence the calcination process, which may affect crystal structure, the morphology and PL intensity. Therefore, the calcination temperatures were varied from 600 to 1000 °C to obtain the crystallization of ZrO_2: 4%Y: 3%Eu. Figure 46 shows the XRD pattern of the ZrO_2: 4%Y: 3%Eu crystal obtained by varying different calcination temperatures, ranging from 600 to 1000 °C. For the calcinations temperature of 600 °C, the diffraction lines of the ZrO_2: 4%Y: 3%Eu crystal indicate a cubic phase. When the calcination temperature was increased, the crystals still remain a cubic phase. However, the diffraction lines at the high temperature are sharper which indicates the increase of crystal size. The crystal size can be estimated by using the Scherrer formular and summarized in Table 3. It was found that the crystal size of ZrO_2: 4%Y: 3%Eu crystal under calcinations temperature at 600, 700, 800, 900 and 1000 °C were 12.9, 12.9, 12.9, 19.4 and 24.2 nm, respectively. The increase of calcinations temperature from 600 to 800 °C hardly affects the crystal sizes. The

crystal size significantly increases when the calcinations temperature was increased above 800 °C, which is probably due to the melting of grain boundary in this temperature range.

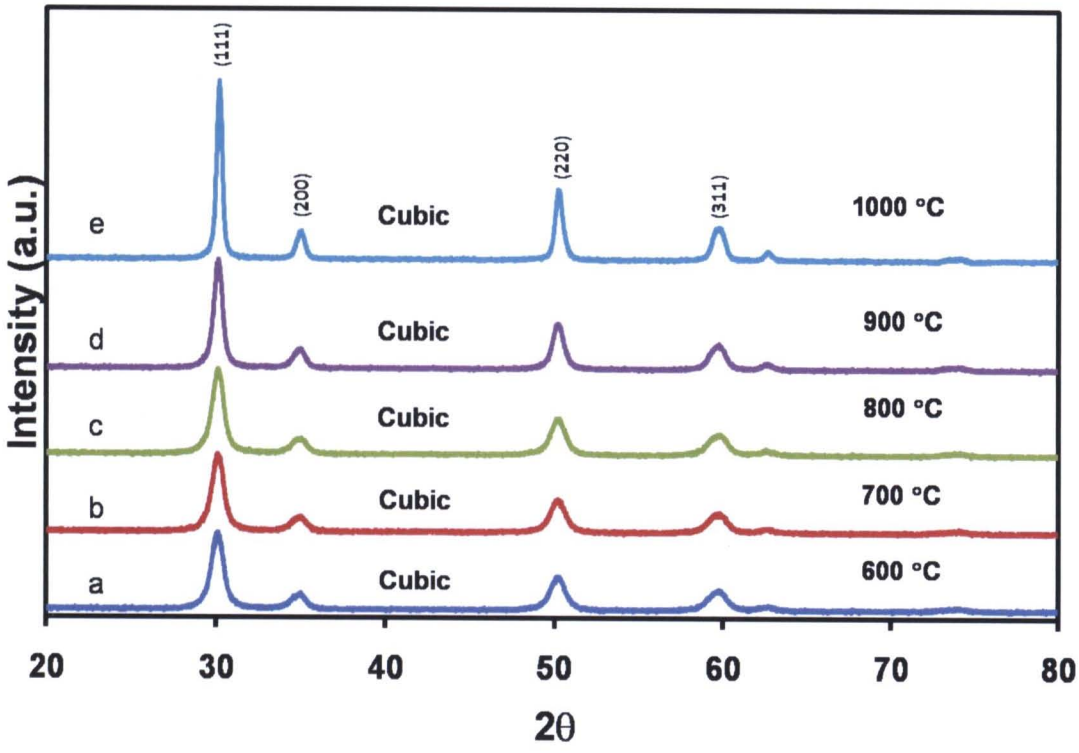

Figure 46 Powder XRD patterns of ZrO_2: 3%Eu: 4%Y crystal under calcination at different temperatures ranging from 600 to 800 °C for 1 h

Table 3 The crystal size of ZrO_2: 3%Eu: 4%Y crystal under calcinations at different temperatures ranging from 600 to 1000 °C for 1 h as calculated from XRD line width

Temperatures (°C)	Crystal size (nm)
600	12.9
700	12.9
800	12.9
900	19.4
1000	24.2

The normalized peaks of the ZrO_2: 4%Y: 3%Eu crystal obtained by varying different calcination temperatures, ranging from 600 to 1000 °C are shown in Figure 47. The increase of calcinations temperature from 600 to 800 °C hardly affects the peak width of crystal. When the calcination temperature was increased to 900 and 1000 °C, the peaks become sharper due to the increasing of crystal size in this temperature range.

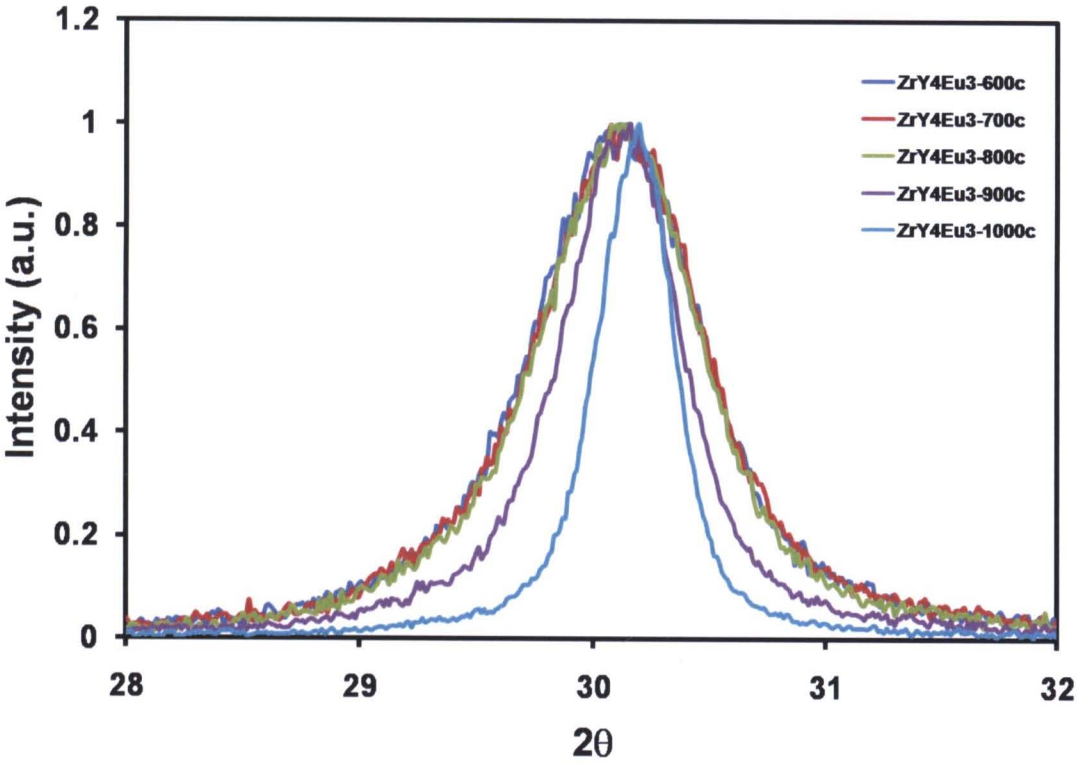

Figure 47 The normalized peak of XRD spectra of ZrO_2: 3%Eu: 4%Y crystal under calcination at different temperatures ranging from 600 to 1000 °C for 1 h

2. Morphology of ZrO_2: 4%Y: 3%Eu crystals

The morphology was investigated by SEM technique. Figure 48 shows the SEM image of ZrO_2: 3%Eu: 4%Y crystals under different calcinations temperature at 600, 700, 800, 900 and 1000 °C for 1 h. The morphologies of all materials are similar. All particles exhibit irregular shape. When calcination temperature was increased, the size of particle becomes smaller. However, it is not trivial to calculate the average particle size because the particles are not well-define.

3. Luminescence properties of ZrO_2: 4%Y: 3%Eu crystals

Figure 49 shows the emission spectra of ZrO_2: 3%Eu: 4%Y crystal under different calcinations temperature at 600, 700, 800, 900 and 1000 °C for 1 h (λ_{ex} = 260 nm). The PL spectrum of sample calcined at 600 °C exhibits a red light emission. When the calcinations temperatures are increased, the samples still emit red color and these PL spectra have similar pattern. The emission peaks correspond to the $^5D_0 - {}^7F_1$ (590 nm) and $^5D_0 - {}^7F_2$ (610 nm) transition of Eu. The PL intensity varies with increasing of calcinations temperature. These results indicate that the calcinations temperature affects on the de-excitation process of the crystals. For the calcination temperature at 800 °C, the PL intensity is highest.

Figure 50 shows the dependence of the emission intensity on the calcinations temperature of ZrO_2: 3%Eu: 4%Y crystal. The integrated PL area of materials was investigated as a function of the calcinations temperature. The peak area was determined as an integral of PL spectrum ranging from 550 to 750 nm. The PL intensity gradually increases upon increasing calcinations temperature from 600 to 800 °C. Further increasing the calcination temperature to 1000 °C results in the decrease of PL intensity. This result may relate to the change of crystal size within the samples. However, the increase of crystal size does not necessary lead to the increase of PL intensity.

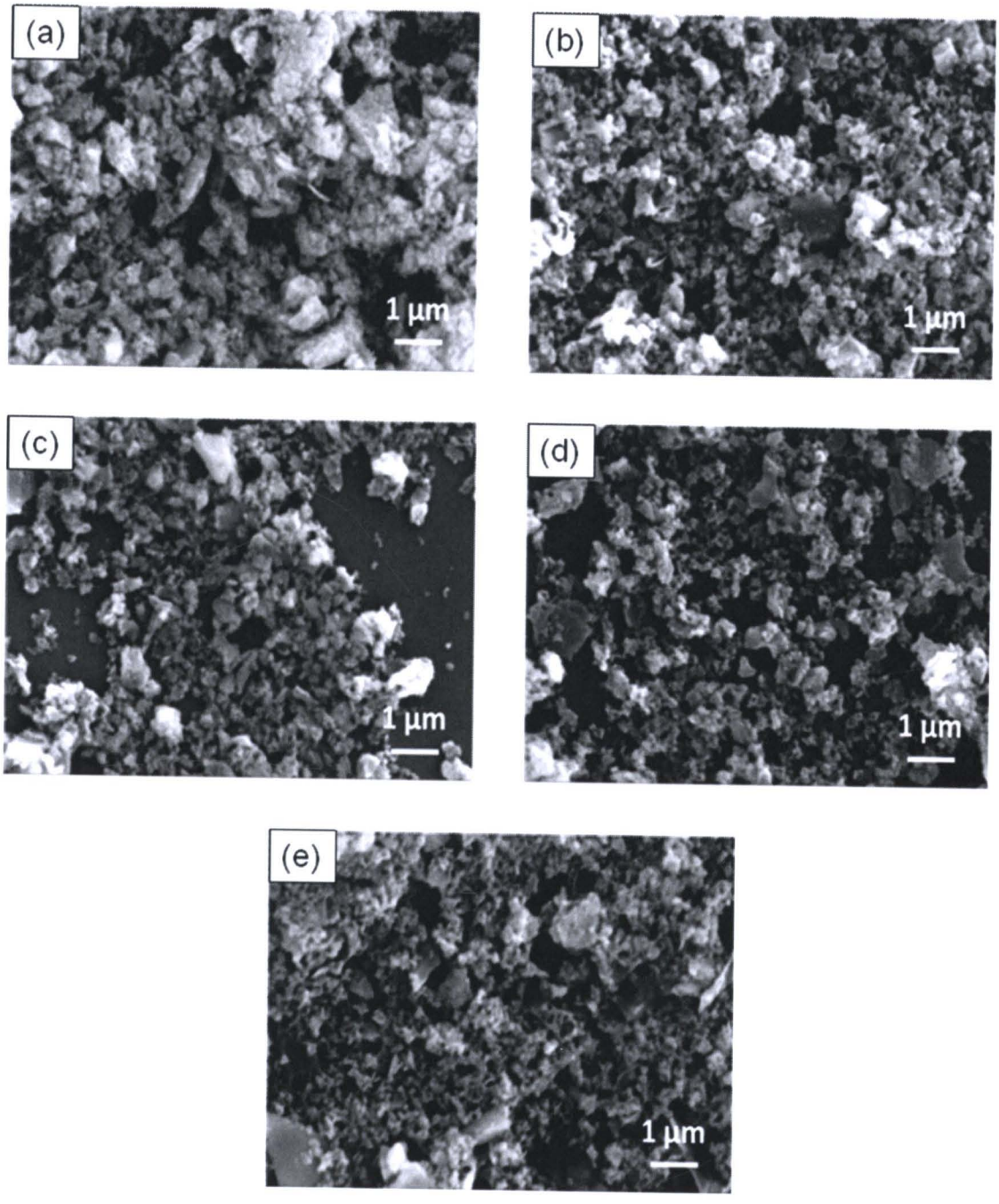

Figure 48 SEM images of ZrO_2: 3%Eu: 4%Y crystal under calcination at different temperatures ranging from 600 to 1000 °C for 1 h

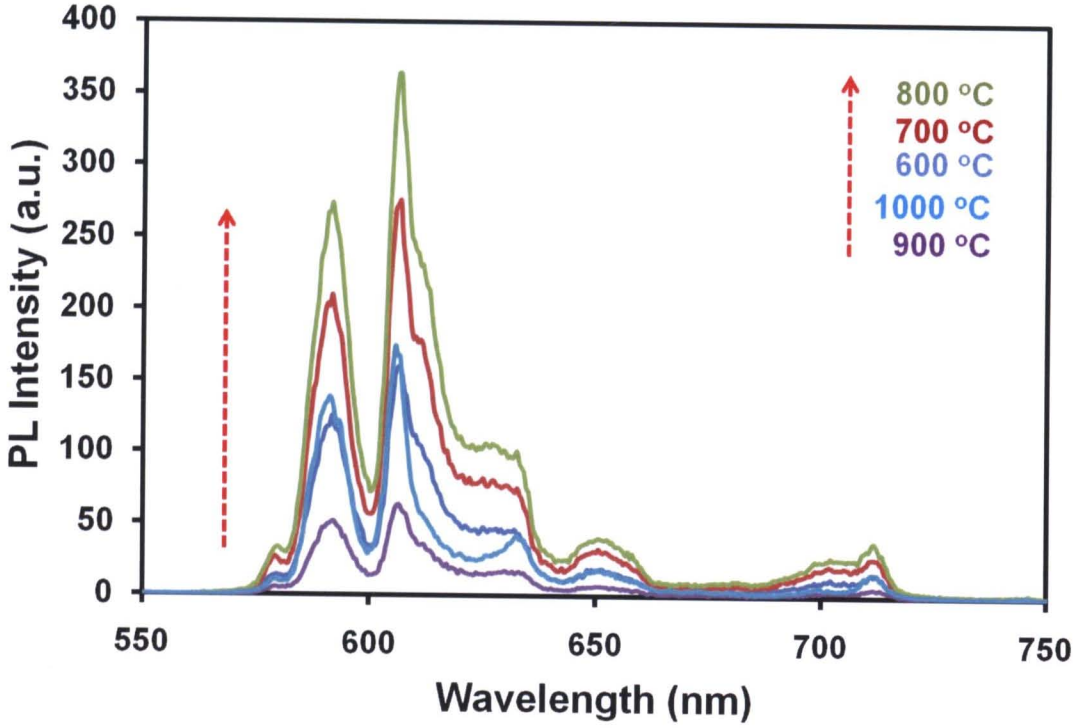

Figure 49 PL emission spectra of ZrO_2: 3%Eu: 4%Y under calcination at different temperatures ranging from 600 to 1000 °C for 1 h

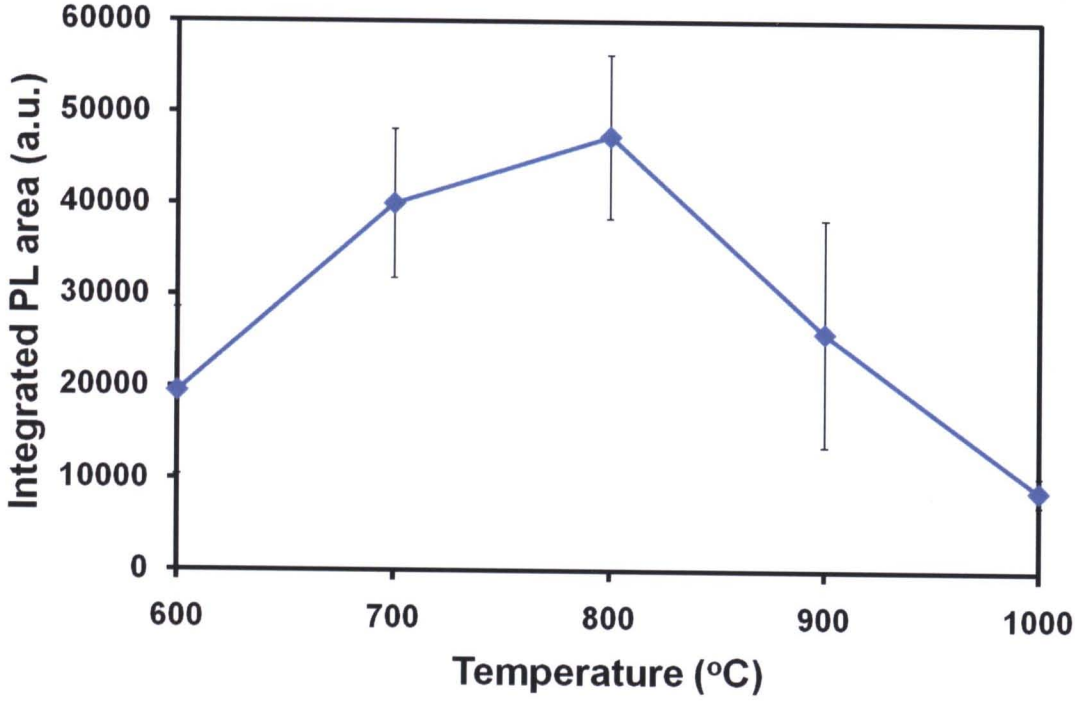

Figure 50 Integrated PL intensities of ZrO_2: 3%Eu: 4%Y under calcinations at different temperatures ranging from 600 to 1000 °C for 1 h

Effect of chelating agents

1. Crystal structure of ZrO_2: 4%Y: 3%Eu crystals

The synthesis of our samples in this study requires chelating agents to induce the complexation with metal ions of the precursors. Therefore, the change of chelating agents is expected to influence the complexing process, which may affect the morphology, crystal structure and PL intensity. Here, we investigate four types of chelating agents including ethylenediaminetetraacetic acid (EDTA), citric acid, malic acid and oxalic acid. These chelating agents have different number of carboxylic group, which is a major functional group for the complexation with the metal ions. Figure 51 shows the XRD pattern of the ZrO_2: 4%Y: 3%Eu crystal obtained by varying different chelating agents under calcination at 800 °C for 1 h. The diffraction line of ZrO_2: 3%Eu: 4%Y crystal obtained by using EDTA is cubic phase. When other chelating agents are used, the crystal structure of materials does not change. These results indicate that the variation of chelating agents does not affect the crystal structure of ZrO_2: 3%Eu: 4%Y. However, the crystal size changes with type of chelating agent. The crystal size of ZrO_2: 4%Y: 3%Eu crystal obtained by using EDTA, citric acid, malic acid and oxalic acid as chelating agents are 16.2, 13.8, 13.8 and 12.1 nm, respectively (see Table 4). The difference of crystal sizes may be ascribed to the binding efficiency of different chelating agents. The EDTA has highest number of carboxyl group compared to the others, which yields the ZrO_2: 4%Y: 3%Eu with largest crystal. However, the complexation process may also depend on the molecular structure of the chelating agents.

The normalized peaks of ZrO_2: 3%Eu: 4%Y crystal obtained by using different chelating agents, citric acid, EDTA, malic acid and oxalic acid are shown in Figure 52. It was found that the normalized peak of ZrO_2: 4%Y: 3%Eu crystal obtained by using EDTA is sharp. The peaks of ZrO_2: 4%Y: 3%Eu crystal obtained by using citric acid, malic acid and oxalic acid become broader, probably due to the decrease of number of carboxyl group in the chelating agents. The broadening of XRD peak corresponds to the decrease of crystal size.

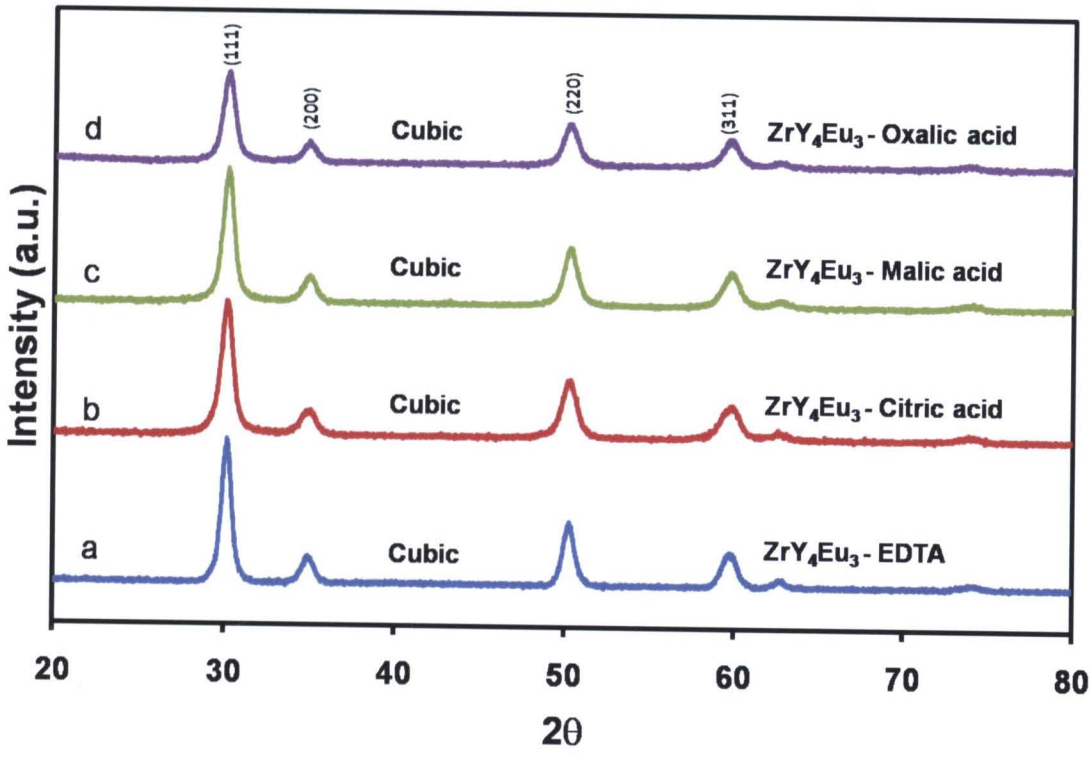

Figure 51 Powder XRD patterns of ZrO_2: 3%Eu: 4%Y crystal obtained by varying different chelating agents under calcination at 800 °C for 1 h

Table 4 The crystal size of ZrO_2: 3%Eu: 4%Y crystal obtained by varying different chelating agents as calculated from XRD line width

Chelating agent	Crystal size (nm)
EDTA	16.2
Citric acid	12.9
Malic acid	13.8
Oxalic acid	12.1

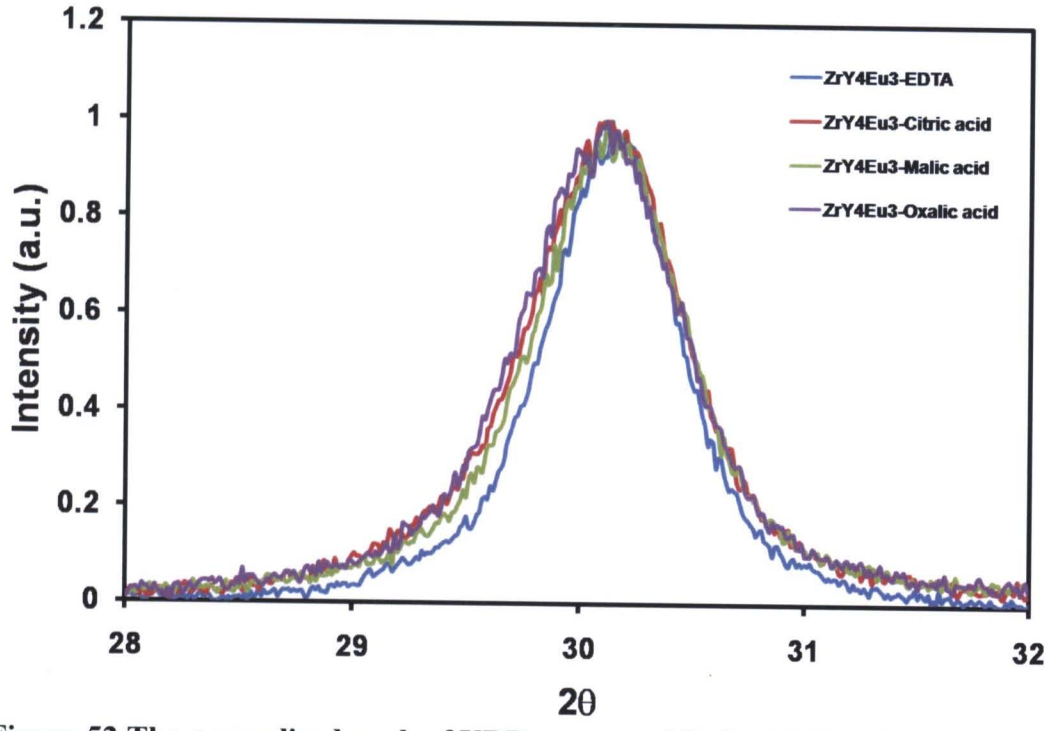

Figure 52 The normalized peak of XRD spectra of ZrO_2: 3%Eu: 4%Y crystal obtained by varying different chelating agents under calcination at 800 °C for 1 h

2. Morphology of ZrO_2: 4%Y: 3%Eu crystals

Figure 53 shows the SEM image of ZrO_2: 3%Eu: 4%Y crystal obtained by using different chelating agents, citric acid, EDTA, malic acid and oxalic acid. All samples exhibit the densely packed particles. The primary size of the particles is less than 100 nm. We do not observe the variation of morphology with type of chelating agents. The results indicate that the structure of chelating agents hardly affects the on morphology of samples.

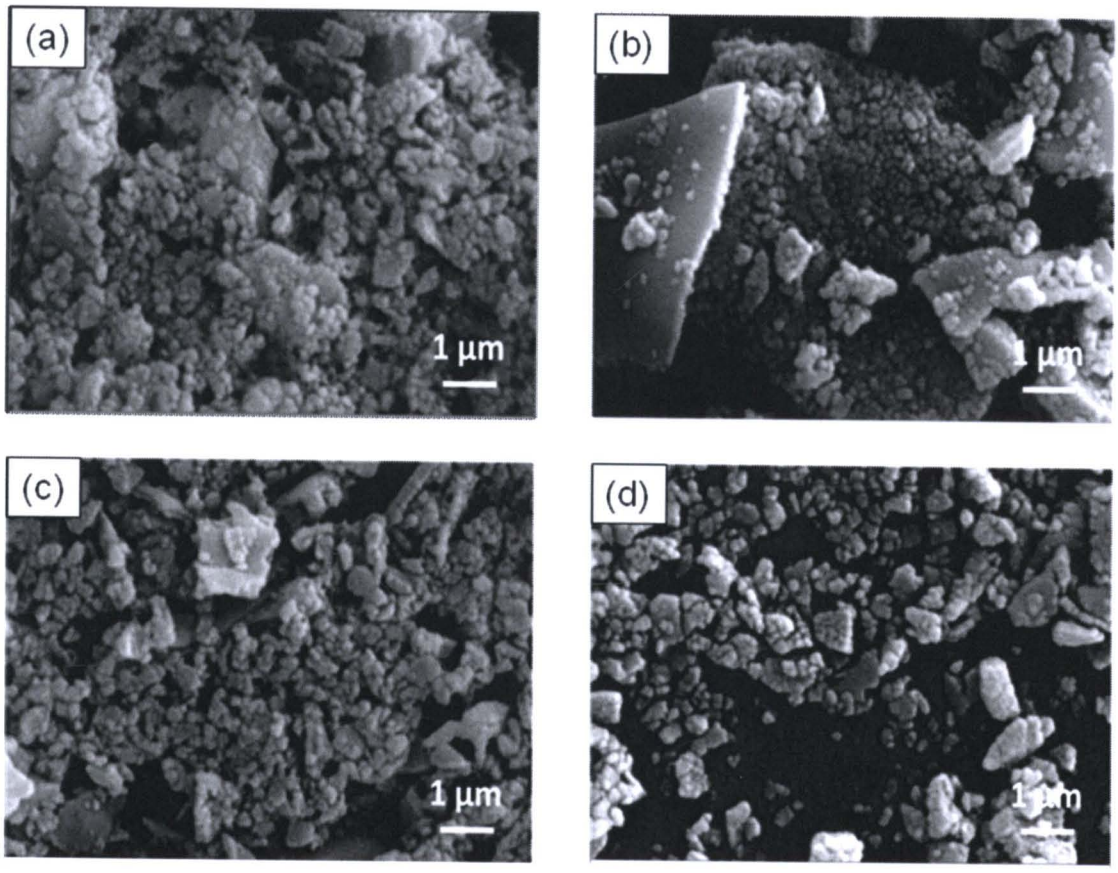

Figure 53 SEM images of ZrO_2: 3%Eu: 4%Y crystal obtained by varying different chelating agents (a) EDTA, (b) citric acid, (c) malic acid and (d) oxalic acid under calcination at 800 °C for 1 h

3. Luminescence properties of ZrO_2: 4%Y: 3%Eu crystals

Figure 54 shows the excitation spectra ZrO_2: 3%Eu: 4%Y crystal obtained by using different chelating agents under calcination at 800 °C for 1 h. The excitation spectra were monitored the emission at 610 nm. The spectrum of ZrO_2: 3%Eu: 4%Y crystal obtained by using EDTA, oxalic acid, malic acid and citric acid consist of a strong band at 229, 246 and 260 nm. The excitation spectrum at wavelength in range of 229 to 260 nm might be ascribed to the host absorption of the oxygen-to-europium charge transfer band (CTB) at UV region. The other weak peaks at about 350 to 480 nm are the direct excitation of the general f-f transitions within the $4f^6$ electron configuration of Eu.

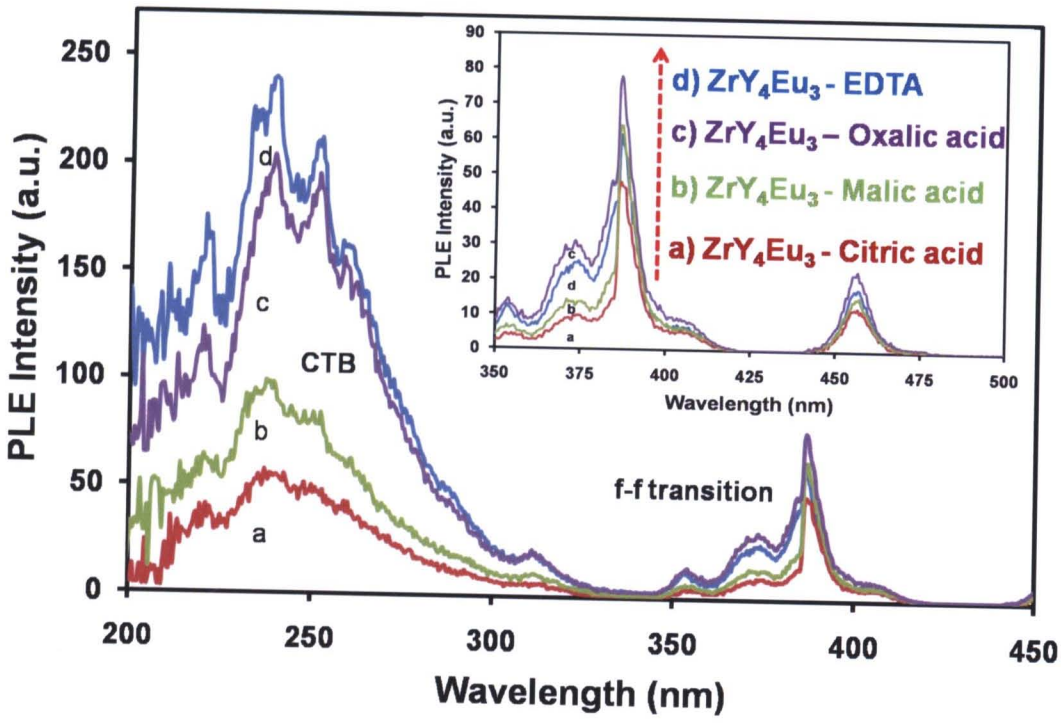

Figure 54 PL excitation spectra of ZrO_2: 3%Eu: 4 %Y crystal obtained by varying different chelating agents under calcination at 800 °C for 1 h

Figure 55 shows the emission spectra of ZrO_2: 3%Eu: 4%Y crystal obtained by using different chelating agents under calcination at 800 °C for 1 h. The spectra were investigated under UV excitation at 260 nm. The PL spectra of the samples exhibit a red luminescent emission. These spectra have similar profile and are composed of $^5D_0 - {}^7F_J$ (J=1, 2, 3, 4) emission lines of Eu. The use of oxalic acid as chelating agent yields the ZrO_2: 3%Eu: 4%Y crystal with highest luminescence efficiency.

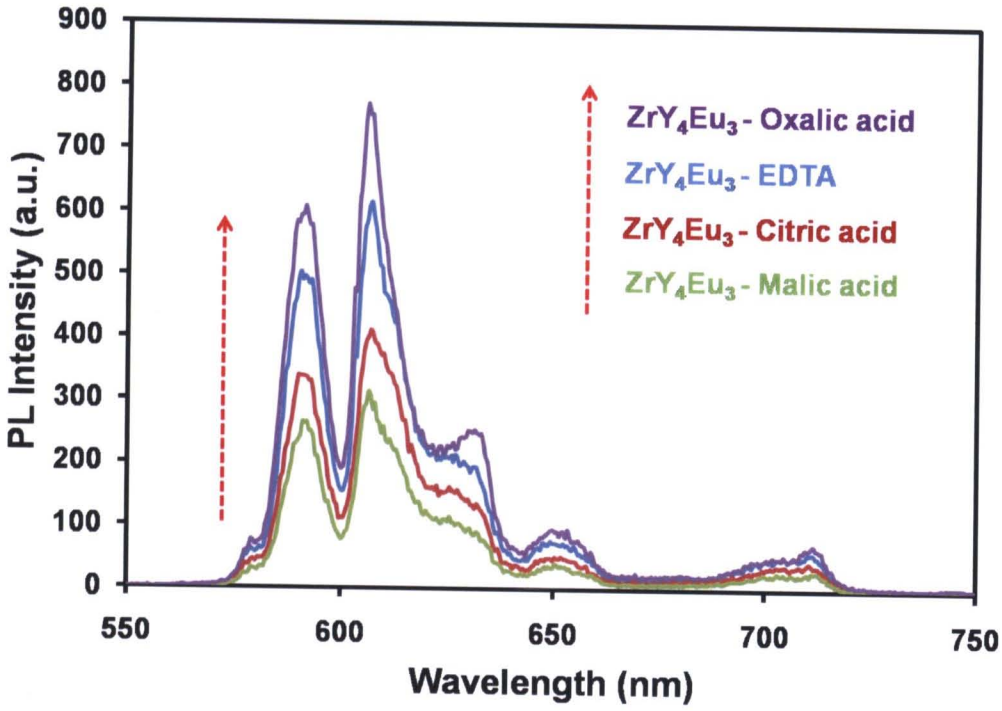

Figure 55 PL emission spectra of ZrO_2: 3%Eu: 4 %Y crystal obtained by varying different chelating agents under calcination at 800 °C for 1 h

To further illustrate the effect of chelating agents on the PL intensity, we plot the graph between PL areas and type of chelating agents as shown in Figure 56. The bar chart clearly shows that the PL intensity of sample obtained by using oxalic acid is highest. The change from oxalic acid to EDTA, malic acid, and citric acid causes systematic decrease of PL intensity. The XRD results indicate the increase of crystal size when the chelating agents are varied in this manner. Therefore, the increase of crystal size may be a major factor that causes the decrease of PL intensity.

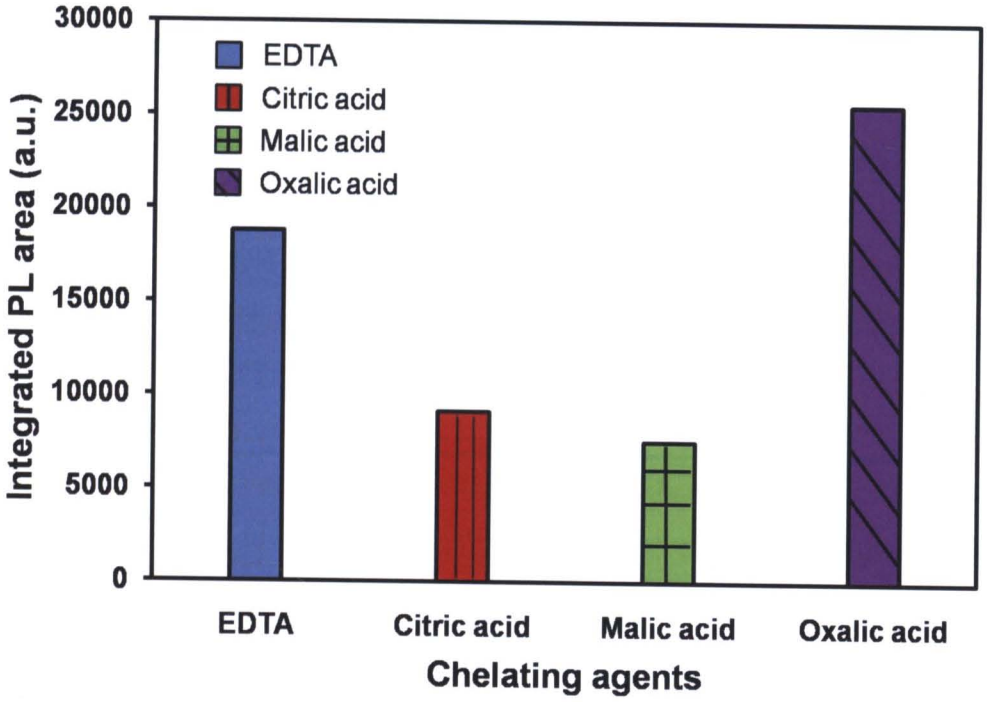

Figure 56 Integrated PL intensities of ZrO_2: 3%Eu: 4%Y crystal obtained by varying different chelating agents under calcination at 800 °C for 1 h

Composite films of ZrO_2: 4%Y: 3%Eu embedded in polyvinyl alcohol (PVA) prepared by drop casting method

1. Luminescence properties

In our earlier discussion, the ZrO_2: 4%Y: 3%Eu crystal can emit a red light and exhibit highest luminescence. In this section, we embed this material in polymeric film of polyvinyl alcohol (PVA). The fabrication in polymeric film allows wider range of applications. Here, 10wt% of PVA and ZrO_2: 4%Y: 3%Eu aqueous solutions with various concentrations at 0.05, 0.1, 0.5, 1 and 2 mol% were mixed thoroughly at 1:1 v/v ratio. The composite films were prepared by drop casting method. The composite films were characterized by photoluminescence and UV-visible absorption spectroscopy. Figure 57 shows the photoluminescence of 10% PVA solutions mixed with various concentrations of ZrO_2: 4%Y: 3%Eu powder ranging from 0.05 to 2 %wt. Prior to the irradiation, all mixed solutions of ZrO_2: 4%Y: 3%Eu in 10% PVA solutions exhibit a white color (see Figure 57a – 57e). When the mixed solutions are excited under UV light, the samples emit a red color. It can be seen that the emission efficiency of the samples increases with increasing of concentration of ZrO_2: 4%Y: 3%Eu powder as shown in Figure 57f – 57j. When the mixed solutions were left at room temperature for about three days, the composite films were obtained as shown Figure 58. The film with low concentration of ZrO_2: 4%Y: 3%Eu has high transparency (see Figure 58a). When the concentrations of ZrO_2: 4%Y: 3%Eu are increased, the film becomes white as shown in Figure 58b – 58e. The surfaces of all films are quite rough, which is due to the heterogeneity of materials during the fabrication process of composite films. When the films are excited under UV light, they still emit a red color (see Figure 58f – 58j). The emission intensity increases with concentration of the ZrO_2: 4%Y: 3%Eu.

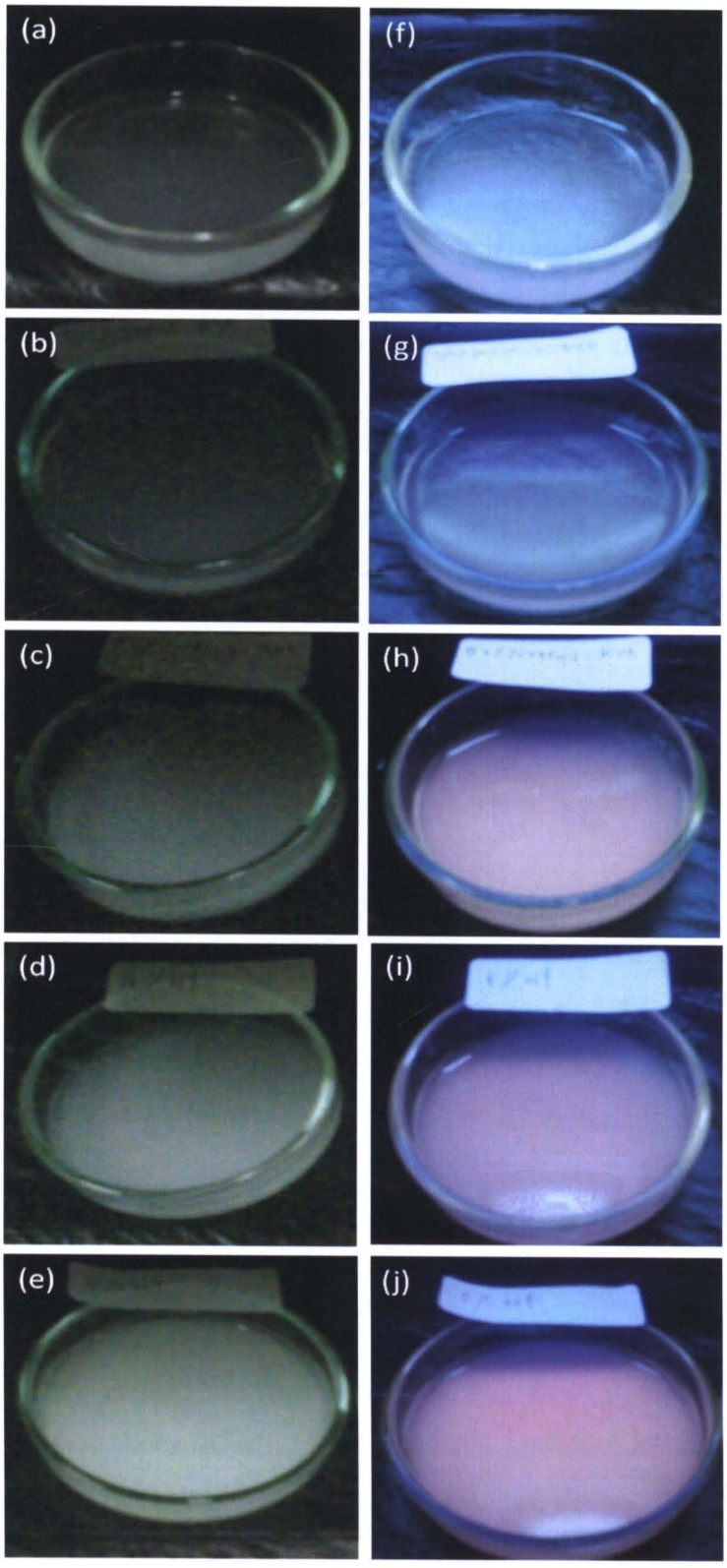

Figure 57 Photographs of the mixed solutions of ZrO_2: 4%Y: 3%Eu embedded in PVA (left) prior to the irradiation and (right) under UV light irradiation

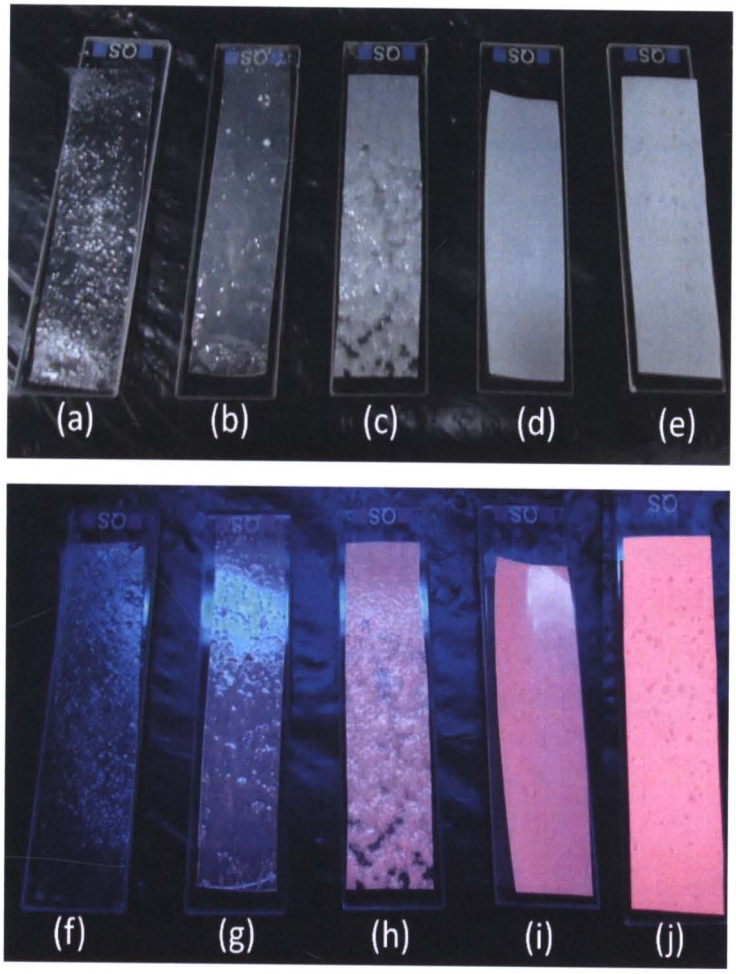

Figure 58 Photographs of composite films of ZrO_2: 4%Y: 3%Eu embedded in PVA (upon) prior to the irradiation and (below) under UV light irradiation. The films were prepared by drop casting method.

The PL emission spectra of composite PVA films mixed with various concentrations of ZrO_2: 4%Y: 3%Eu ranging from 0.05 to 2 %wt are shown in Figure 59. The spectra of composite films exhibit a red luminescent emission. These PL spectra exhibited similar pattern and corresponded to the $^5D_0 - {}^7F_1$ (590 nm) and $^5D_0 - {}^7F_2$ (610 nm) emission lines of Eu. The emission intensity of composite films systematically increases with increasing concentration of ZrO_2: 4%Y: 3%Eu. The results indicate that ZrO_2: 4%Y: 3%Eu powder can be utilized as a composite PVA film.

To further illustrate the effect of ZrO_2: 4%Y: 3%Eu embedded in composite PVA films on the PL intensity, we plotted the graph between PL areas and

concentration of ZrO_2: 4%Y: 3%Eu as shown in Figure 60. The PL areas were integrated from 550 to 750 nm. The plot clearly shows that the PL intensity increases upon increasing concentrations of ZrO_2: 4%Y: 3%Eu. However, the plot does not exhibit linear relationship according Beer's Law. The deviation is clear when the concentration of ZrO_2: 4%Y: 3%Eu is at 1 and 2 %. We suggest that the deviation from linear relationship is due to the concentration quenching within the system.

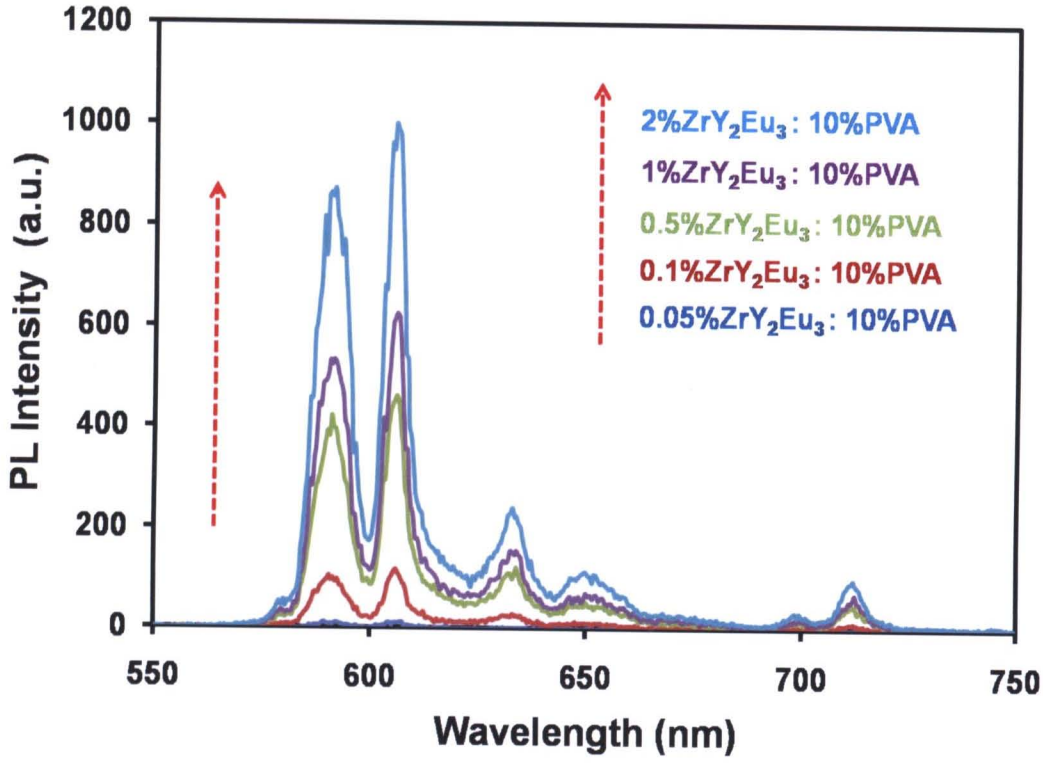

Figure 59 PL emission spectra of composite films of ZrO_2: 4%Y: 3%Eu embedded in PVA by drop casting method

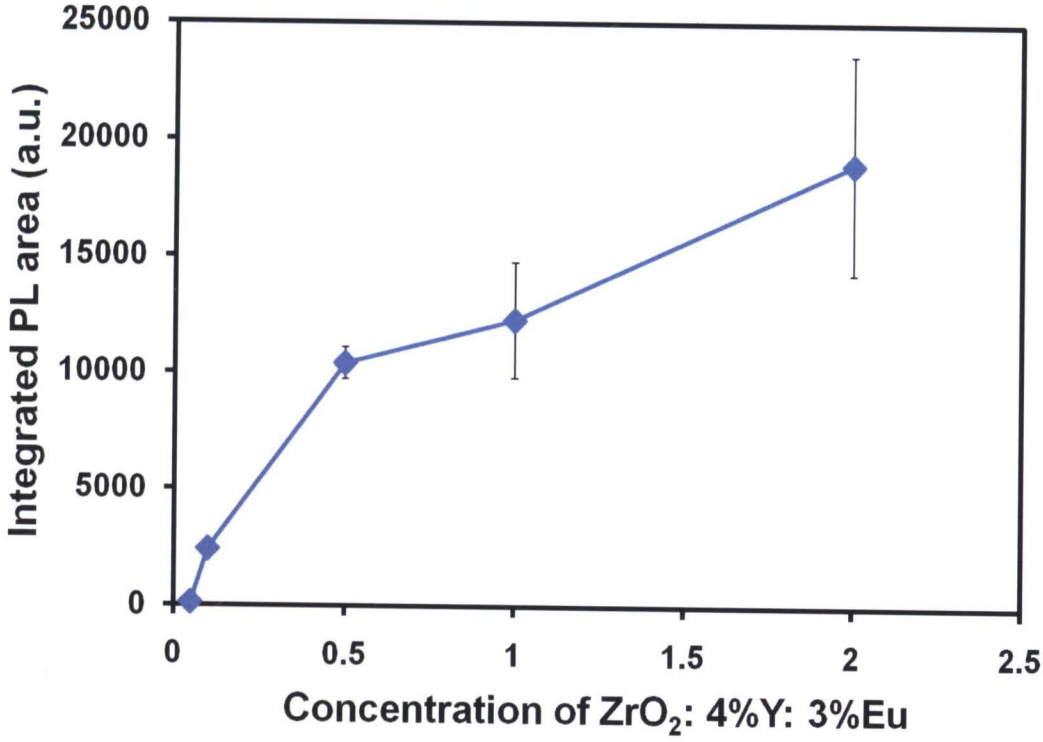

Figure 60 Integrated PL intensities of composite films of ZrO_2: 4%Y: 3%Eu embedded in PVA by drop casting method

2. Transparent properties

The transparent properties were studied by using the UV spectroscopy technique. The transmission spectra of composite film of PVA mixed with various concentrations of ZrO_2: 4%Y: 3%Eu ranging from 0.05 to 2 %wt is shown in Figure 61. The films with low concentration of ZrO_2: 4%Y: 3%Eu are quite transparent. The drop of transmission intensity in the UV range is probably due to the absorption of ZrO_2. When the concentration of ZrO_2: 4%Y: 3%Eu is increased above 0.5 wt%, the transmission intensity decreases significantly. These films are opaque to naked eyes.

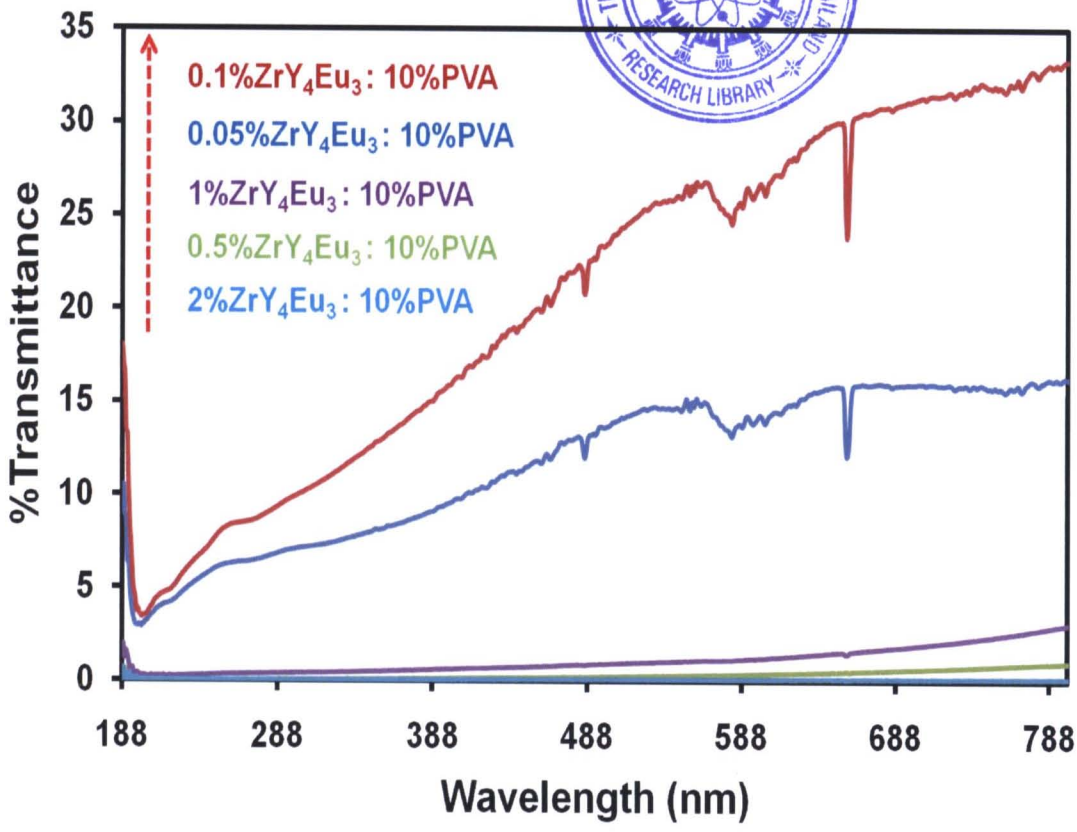

Figure 61 Transmission spectra of composite films of ZrO_2: 4%Y: 3% embedded in PVA by drop casting method

Composite films of ZrO_2: 4%Y: 3%Eu embedded in polyvinyl alcohol (PVA) prepared by spin casting method

1. Luminescence properties

As mentioned above, the composite films of ZrO_2: 4%Y: 3%Eu embedded in PVA prepared by drop casting method exhibit quite rough surface. This is due to the heterogeneity of materials during the fabrication process of composite films. Therefore, we improve this problem with the preparation by spin casting method. This method is easy, cheap and provides homogeneous sample. The film thickness can also be controlled by adjusting spinning rate and polymer concentration. In this section, PVA and ZrO_2: 4%Y: 3%Eu aqueous solutions with various concentrations at 0.05, 0.1, 0.5, 1 and 2 mol% were mixed thoroughly at 1:1 v/v ratio. When the mixed solutions were deposited onto spinning substrates, the composite films were obtained.

The composite films are smoother and thinner than the films obtained from drop casting method.

Figure 62 shows the excitation spectra for composite PVA films mixed with various concentrations of ZrO_2: 4%Y: 3%Eu by monitoring the emission at 610 nm. The excitation spectrum of 1 mol% of ZrO_2: 4%Y: 3%Eu embedded in PVA consists of a strong band at 229 and 246 nm similar to the excitation spectrum of ZrO_2: 4%Y: 3%Eu crystal (see in Figure 62a). The increasing of ZrO_2: 4%Y: 3%Eu in PVA to 2 mol% slightly affect the pattern of spectra (see in Figure 62b). These spectra might be ascribed to the host absorption of the oxygen-to-europium charge transfer band (CTB) at UV region. The other weak peaks at about 350 to 480 nm are due to the general f-f transitions within the $4f^6$ electron configuration of Eu.

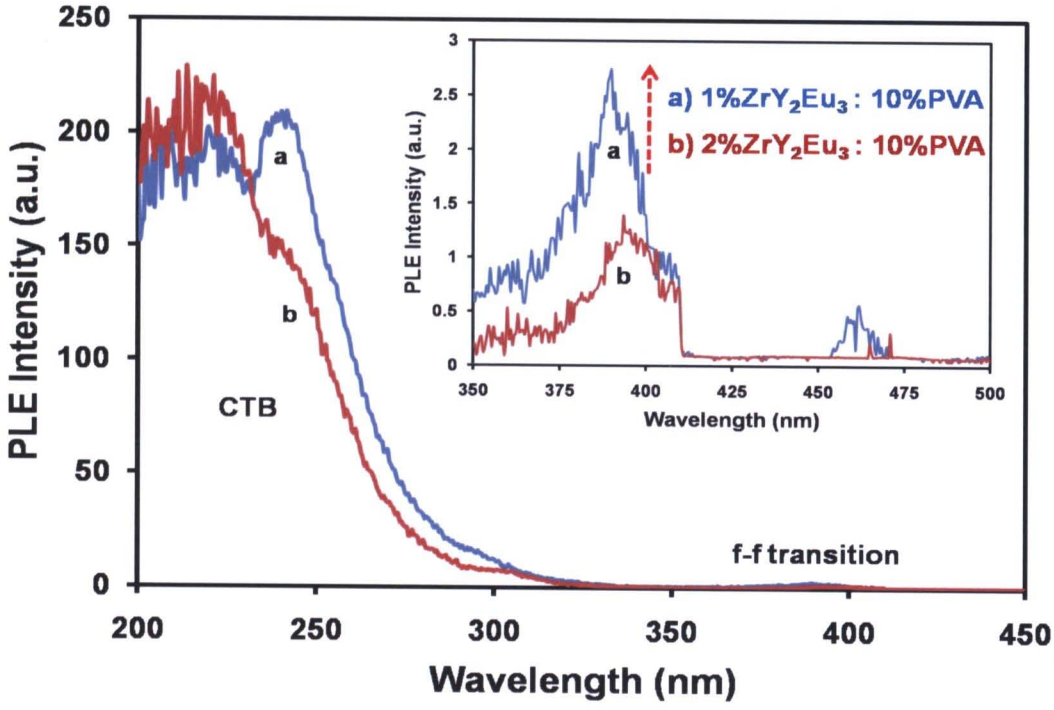

Figure 62 PL excitation spectra of composite films of ZrO_2: 4%Y: 3%Eu embedded in PVA by spin casting method

Figure 63 shows the emission spectra of composite films of ZrO_2: 4%Y: 3%Eu embedded in PVA under UV excitation at wavelength of 260 nm. The emission spectra still exhibits a red luminescent emission which corresponds to the $^5D_0 - {}^7F_1$ (590 nm) and $^5D_0 - {}^7F_2$ (610 nm) transition of Eu. The emission intensity is apparently

intensifying with increasing concentration of ZrO_2: 4%Y: 3%Eu. Therefore, the fabrication of composite films by using spin casting technique provides luminescence properties as same as the films preparation by using drop casting technique.

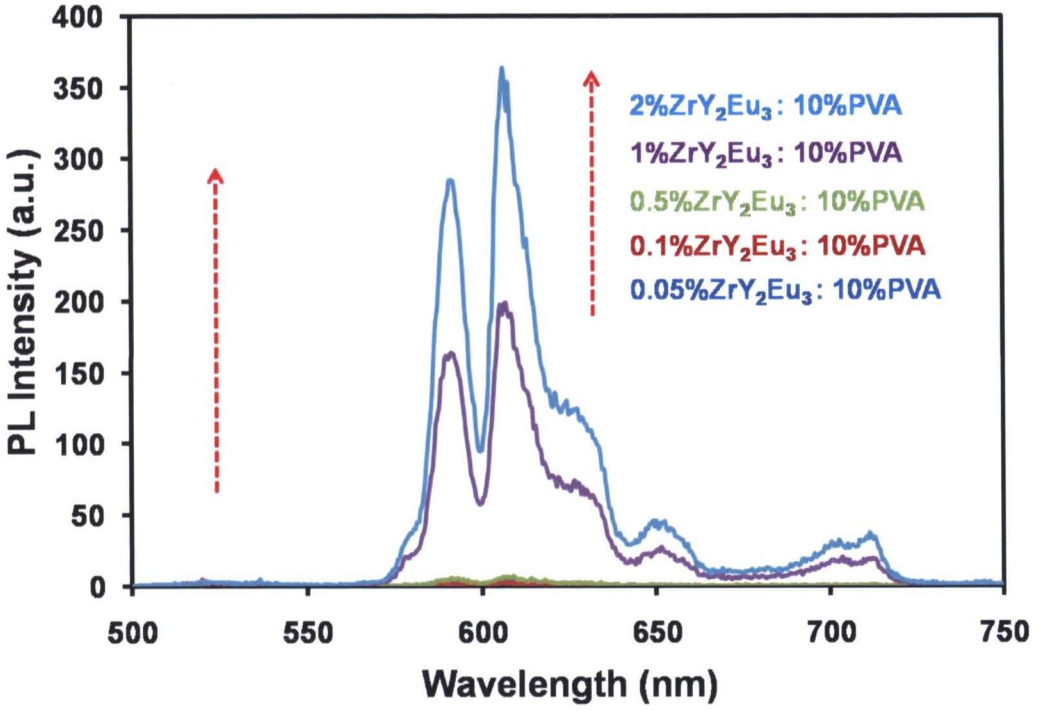

Figure 63 PL emission spectra of composite films of ZrO_2: 4%Y: 3%Eu embedded in PVA by spin casting method

Figure 64 shows the photoluminescence of composite films of ZrO_2: 4%Y: 3%Eu embedded in PVA with various concentrations of ZrO_2: 4%Y: 3%Eu powder ranging from 0.05 to 2 %wt by naked eyes. Prior to the irradiation, the film with low concentration of ZrO_2: 4%Y: 3%Eu has high transparency (see Figure 64a-64c). When the concentrations of ZrO_2: 4%Y: 3%Eu are increased, the film becomes white as shown in Figure 64d – 64e. When the composite films are excited under UV light, the samples emit a red color. It can be seen that the emission efficiency of the samples increases with increasing of concentration of ZrO_2: 4%Y: 3%Eu powder as shown in Figure 64f – 64j.

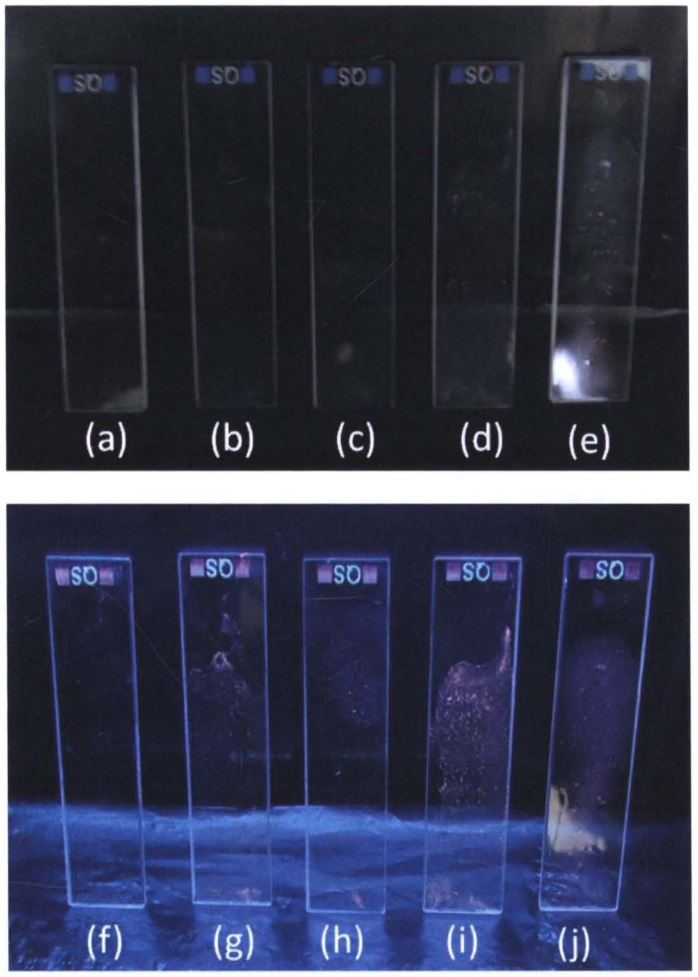

Figure 64 Photographs of composite films of ZrO_2: 4%Y: 3%Eu embedded in PVA (upon) prior to the irradiation and (below) under UV light irradiation. The films were prepared by spin casting method.

2. Transparent properties

Figure 65 shows the transmission spectra of composite films of PVA mixed with different concentration of ZrO_2: 4%Y: 3%Eu ranging from 0.05 to 2 mol%. All composite films of ZrO_2: 4%Y: 3%Eu are quite transparent. When the concentration of ZrO_2: 4%Y: 3%Eu is increased, the transmission intensity decreases significantly.

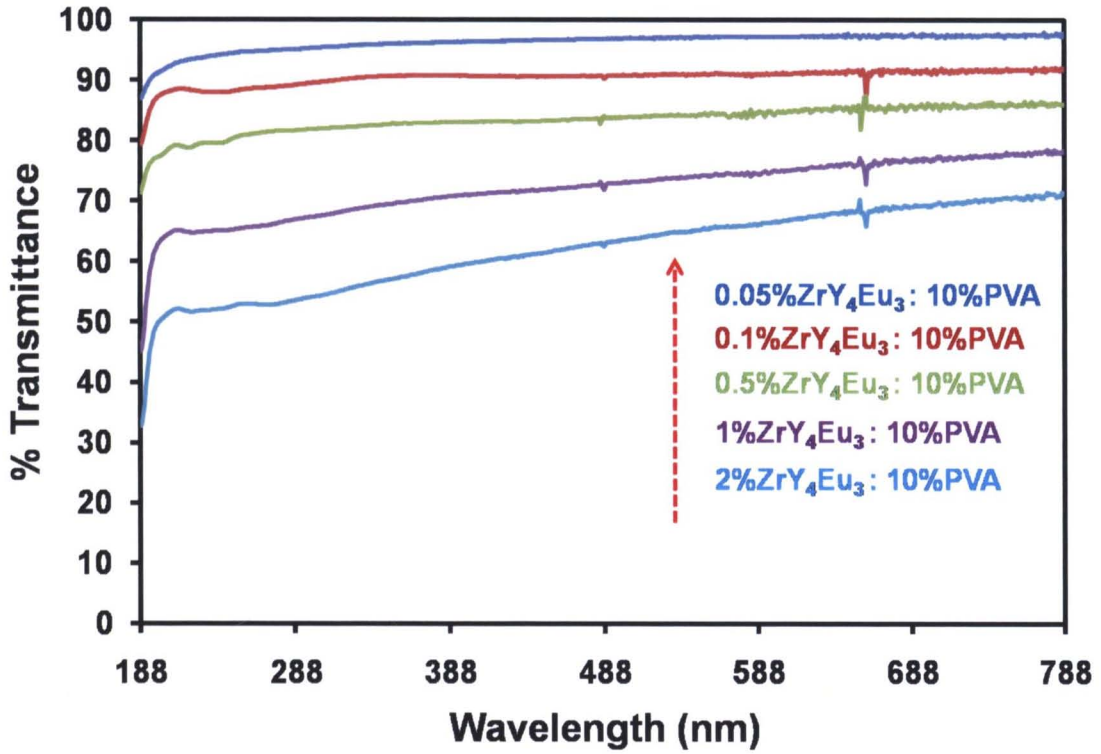

Figure 65 Transmission spectra of composite film of ZrO_2: 4%Y: 3%Eu embedded in PVA by spin casting method

Composite films of ZrO_2: 4%Y: 3%Eu embedded in different polymers prepared by spin casting method

In our study, we make further effort to prepare composite films of ZrO_2: 4%Y: 3%Eu embedded in different polymers by using spin casting method. The polymers included polystyrene or PS, poly (methyl methacrylate) or PMMA and poly acrylic acid or PAA. These polymers were dissolved into different solvents which depend on solubility of each polymer as described in Chapter III. The composite films of 0.5 wt% of ZrO_2: 4%Y: 3%Eu embedded in 10 wt% of different polymers were prepared.

1. Luminescence properties

Figure 66 shows the excitation spectra for ZrO_2: 4%Y: 3%Eu embedded in different polymers by monitoring the emission at 610 nm. The excitation spectra of ZrO_2: 4%Y: 3%Eu embedded in PVA, PAA and PMMA composite films consist of a strong band at 246 nm (see Figure 66a-66c). When ZrO_2: 4%Y: 3%Eu is embedded in PS composite films, the spectrum exhibits peaks at 246 and 276 nm as shown in

Figure 66d. These excitation spectra still consist of the CTB band of host absorption and the direct excitation of the general f-f transitions within the $4f^6$ electron configuration of Eu.

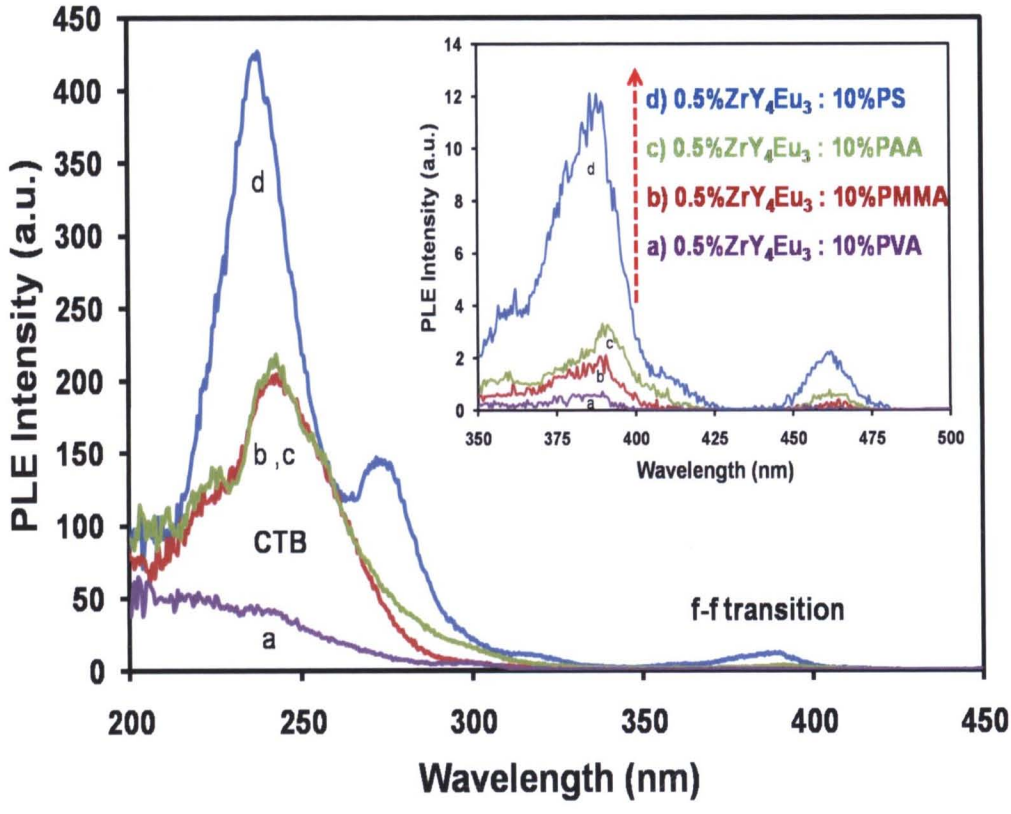

Figure 66 PL excitation spectra of composite films of ZrO_2: 4%Y: 3%Eu embedded in different polymers by spin casting method

PL spectra of composite films of ZrO_2: 4%Y: 3%Eu embedded in different polymers are shown in Figure 67. The samples were excited under UV excitation at wavelength of 260 nm. It is clearly seen that the PL spectra exhibit a red luminescent emission and corresponds to the $^5D_0 - {}^7F_1$ (590 nm) and $^5D_0 - {}^7F_2$ (610 nm) transition of Eu. The highest emission intensity of the composite films is detected from ZrO_2: 4%Y: 3%Eu embedded in PS as shown in Figure 68. This result indicates that the structure of polymer affects the luminescence efficiency of materials. This observation is probably due to the difference of polymer polarity, which affects the de-excitation pathways of electrons within the materials.

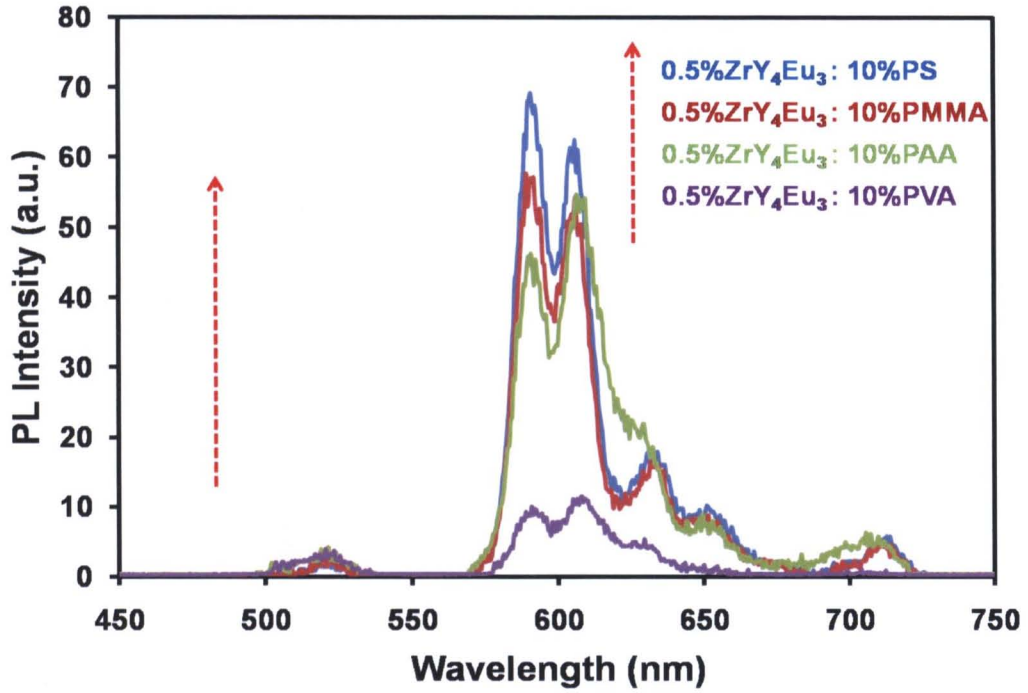

Figure 67 PL emission spectra of composite films of ZrO_2: 4%Y: 3%Eu embedded in different polymers by spin casting method

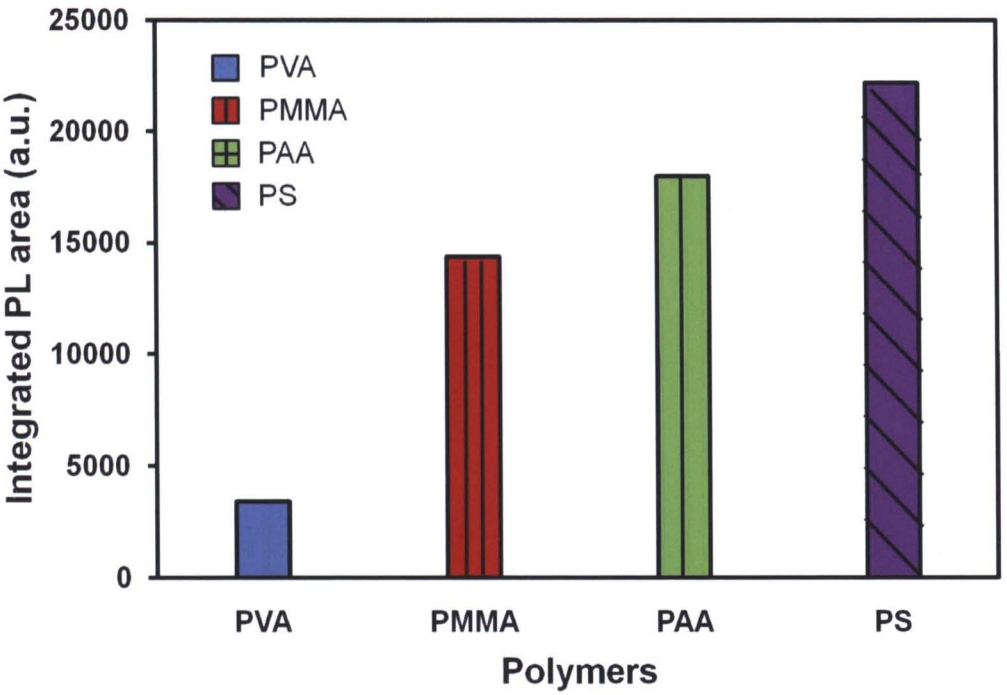

Figure 68 Integrated PL intensities of composite films of ZrO_2: 4%Y: 3%Eu embedded in different polymers by spin casting method

Figure 69 shows the photoluminescence of composite films of ZrO_2: 4%Y: 3%Eu embedded in PVA, PAA, PMMA and PS by naked eyes. Prior to the irradiation, the composited films of ZrO_2: 4%Y: 3%Eu embedded in PVA and PAA has high transparency (see Figure 69a, 69b). When the composited films of ZrO_2: 4%Y: 3%Eu is embedded in PMMA and PS, the films are opaque to naked eyes as shown in Figure 69c, 69d. When excited under UV light, the composited films of ZrO_2: 4%Y: 3%Eu embedded in PVA, PAA, PMMA and PS emit red color (see Figure 69e- 69h). However, the emission efficiency of the samples cannot be clearly seen by naked eyes.

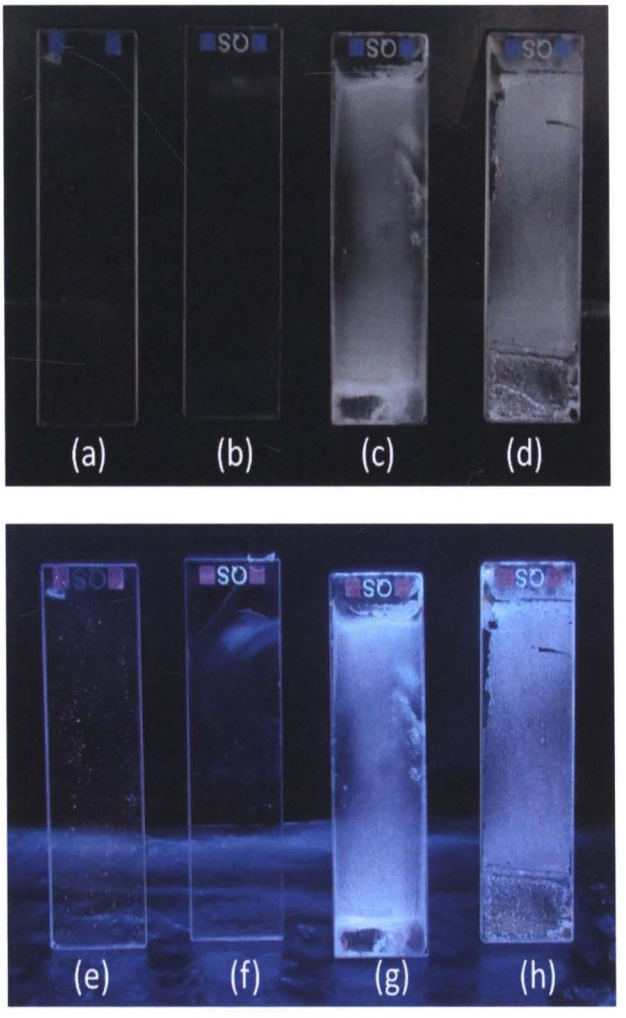

Figure 69 Photographs of composite films of ZrO_2: 4%Y: 3%Eu embedded in different polymers by spin casting method (upon) prior to the irradiation and (below) under UV light irradiation

2. Transparent properties

Figure 70 shows the transmission spectra of composite films of ZrO_2: 4%Y: 3%Eu embedded in different polymers. All composite films of ZrO_2: 4%Y: 3%Eu in PVA and PAA composite films are quite transparent. When ZrO_2: 4%Y: 3%Eu is embedded in PS and PMMA composite films, the transmission intensity decreases significantly.

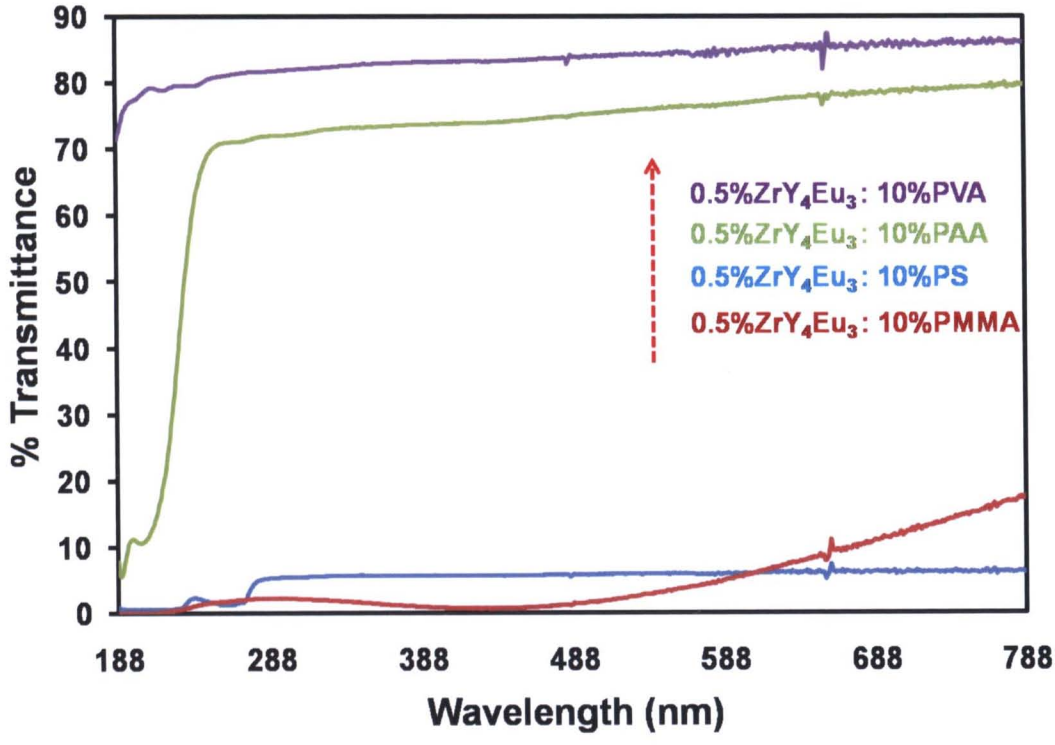

Figure 70 Transmission spectra of composite films of ZrO_2: 4%Y: 3%Eu embedded in different polymers by spin casting method